Journal of Proteomics 187 (2018) 243–259

Contents lists available at ScienceDirect

Journal of Proteomics

journal homepage: www.elsevier.com/locate/jprot

Catabolism of phenylacetic acid in *Penicillium rubens*. Proteome-wide analysis in response to the benzylpenicillin side chain precursor

Mohammad-Saeid Jami[a,b], Juan-Francisco Martín[c,*], Carlos Barreiro[a], Rebeca Domínguez-Santos[a,c], María-Fernanda Vasco-Cárdenas[a,c], María Pascual[a], Carlos García-Estrada[a,d,**]

[a] INBIOTEC, Instituto de Biotecnología de León, Avda. Real n°. 1, Parque Científico de León, 24006 León, Spain
[b] Cellular and Molecular Research Center, Basic Health Sciences Institute, Shahrekord University of Medical Sciences, Shahrekord, Iran
[c] Área de Microbiología, Departamento de Biología Molecular, Universidad de León, Campus de Vegazana s/n, 24071 León, Spain
[d] Departamento de Ciencias Biomédicas, Facultad de Veterinaria, Universidad de León, Campus de Vegazana s/n, 24071 León, Spain

ARTICLE INFO

Keywords:
Phenylacetic acid
Benzylpenicillin
2-hydroxyphenylacetate
Phenylacetate hydroxylase
Proteomics
Penicillium rubens

ABSTRACT

Biosynthesis of benzylpenicillin in filamentous fungi (e.g. *Penicillium chrysogenum* - renamed as *Penicillium rubens*- and *Aspergillus nidulans*) depends on the addition of CoA-activated forms of phenylacetic acid to isopenicillin N. Phenylacetic acid is also detoxified by means of the homogentisate pathway, which begins with the hydroxylation of phenylacetic acid to 2-hydroxyphenylacetate in a reaction catalysed by the *pahA*-encoded phenylacetate hydroxylase. This catabolic step has been tested in three different penicillin-producing strains of *P. rubens* (*P. notatum*, *P. chrysogenum* NRRL 1951 and *P. chrysogenum* Wisconsin 54–1255) in the presence of sucrose and lactose as non-repressing carbon sources. *P. chrysogenum* Wisconsin 54–1255 was able to accumulate 2-hydroxyphenylacetate at late culture times. Analysis of the *P. rubens* genome showed the presence of several PahA homologs, but only Pc16g01770 was transcribed under penicillin production conditions. Gene knock-down experiments indicated that the protein encoded by Pc16g01770 seems to have residual activity in phenylacetic acid degradation, this catabolic activity having no effect on benzylpenicillin biosynthesis. Proteome-wide analysis of the Wisconsin 54–1255 strain in response to phenylacetic acid revealed that this molecule has a positive effect on some proteins directly related to the benzylpenicillin biosynthetic pathway, the synthesis of amino acid precursors and other important metabolic processes.

Significance: The adaptive response of *Penicillium rubens* to benzylpenicillin production conditions remains to be fully elucidated. This article provides important information about the molecular mechanisms interconnected with phenylacetate (benzylpenicillin side chain precursor) utilization and penicillin biosynthesis, and will contribute to the understanding of the complex physiology and adaptation mechanisms triggered by *P. rubens* (*P. chrysogenum* Wisconsin 54–1255) under benzylpenicillin production conditions.

1. Introduction

Since Fleming's fortuitous discovery of penicillin ninety years ago, constant efforts have been made by the scientific community from industry and academia in order to improve penicillin titers. This has been achieved mainly by industrial strain improvement programs, where selected strains have been subjected during the last decades to several rounds of radioactive and chemical mutagenesis, thus reaching product titers and productivities three orders of magnitude higher than those provided by the ancestor strains [1]. The fungal strain producing the antimicrobial agent penicillin was initially identified by Fleming and colleagues as *Penicillium rubrum*, which was later re-identified as *Penicillium notatum* and finally placed in synonymy with *Penicillium chrysogenum*. However, this nomenclature has been recently reconsidered, leading to the conclusion that Fleming's original strain, the full genome sequenced strain *P. chrysogenum* Wisconsin 54–1255 and its ancestor strain *P. chrysogenum* NRRL 1951 (wild-type), are in fact *Penicillium rubens* [2]. Although all these strains are now classified as *P. rubens*, for the sake of clarity the old names *P. notatum*, *P. chrysogenum* Wisconsin 54–1255 and NRRL-1951 are also used in this article, since hundreds of

* Corresponding author.
** Corresponding author at: INBIOTEC, Instituto de Biotecnología de León, Avda. Real n°. 1, Parque Científico de León, 24006 León, Spain.
E-mail addresses: jf.martin@unileon.es (J.-F. Martín), carlos.garcia@inbiotec.com, c.gestrada@unileon.es (C. García-Estrada).

https://doi.org/10.1016/j.jprot.2018.08.006
Received 14 May 2018; Received in revised form 17 July 2018; Accepted 4 August 2018
Available online 06 August 2018
1874-3919/

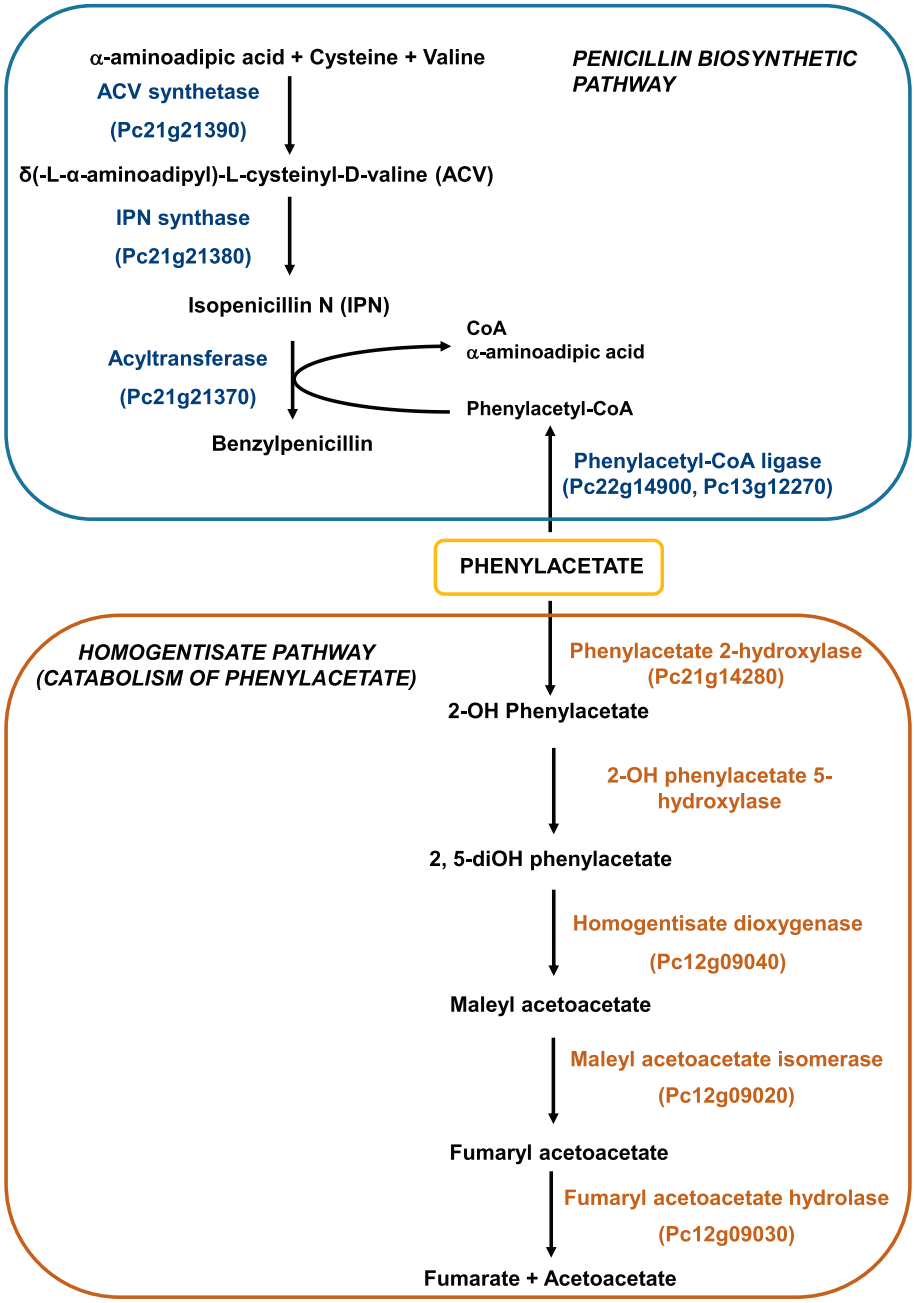

Fig. 1. Metabolic routes of phenylacetic acid in *P. rubens*: penicillin biosynthetic pathway (upper chart) and homogentisate pathway (lower chart).

references using the old names have been published.

Much of the efforts made by the scientific community have focused on the biochemical and genetic characterization of the penicillin biosynthetic pathway [3] (Fig. 1), which is compartmentalized between cytosol and peroxisomes (for reviews see [4, 5]). It starts with the nonribosomal condensation of L-α-aminoadipic acid, L-cysteine and L-valine by means of the nonribosomal peptide synthetase L-δ(α-aminoadipyl)-L-cysteinyl-D-valine (ACV) synthetase (ACVS), which is a very large multifunctional protein (MW 426 kDa). This protein is encoded by the single structural 11-kbp *pcbAB* gene. Next, in a reaction catalysed by the isopenicillin N (IPN) synthase or cyclase (encoded by the *pcbC* gene), the ACV undergoes the oxidative ring closure of the tripeptide. This leads to the formation of the bicyclic structure (penam nucleus) of IPN in the cytosol. In the last step of the penicillin biosynthetic pathway, the α-aminoadipyl side chain of IPN is replaced inside peroxisomes by a hydrophobic side chain activated as thioester with CoA. In the case of benzylpenicillin, the side chain precursor is phenylacetic acid, which is activated in the form of phenylacetyl CoA. Replacement is catalysed by the *penDE*-encoded acyl-CoA: IPN acyltransferase (IAT), which is synthesized as a 40-kDa precursor protein (proIAT) that undergoes self-processing between residues Gly102 and Cys103. Therefore, the active protein is a heterodimer comprising two subunits: α (11 kDa, corresponding to the N-terminal fragment) and β (29 kDa, corresponding to the C-terminal region). Activation of the side chain precursor is achieved by means of aryl CoA-ligases. At least three aryl-CoA ligases, encoded by the *phl, phlB* (*aclA*) and *phlC* genes, respectively, have been reported to activate phenylacetic acid [6–9]. However, direct contribution to penicillin biosynthesis has only been described in the case of the phenylacetyl CoA ligase encoded by the *phl* gene [6].

Research has also been focused on the characterization of the modifications introduced by industrial strain improvement programs.

Amplification of the penicillin gene cluster is well documented in many of the improved penicillin producers, which contain several copies of this cluster (e.g. the AS-P-78 strain contains 5 or 6 copies) [10]. Microbodies (peroxisomes), the organelles where activation of the side chain and its incorporation to the IPN molecule occur, are more abundant in high-producer strains [11, 12]. Genome and transcriptome analyses have also revealed that transcription of genes involved in the biosynthesis of the penicillin amino acid precursors, as well as of those genes encoding microbody proteins, was higher in the high-producer strain DS17690 [12]. More recently, proteomics studies concluded that the increase in penicillin production along the industrial strain improvement program was a consequence of complex metabolic reorganizations, and suggested that energetic burden, redox metabolism or the supply of precursors are crucial for the biosynthesis of this antibiotic [13].

Besides this background knowledge, it is well known that the homogentisate pathway for the catabolism of phenylacetic acid (the side chain precursor in the biosynthesis of benzylpenicillin) to fumarate and acetoacetate (Fig. 1) is diminished in Wisconsin 54–1255, and presumably, in derived strains as well [14, 15]. Phenylacetic acid is a weak acid that is toxic to cells depending on its concentration and culture pH. This compound can be metabolized in *P. rubens* (*P. chrysogenum*) and *Aspergillus nidulans* (another filamentous fungus with the ability to biosynthesize benzylpenicillin) through at least two routes; incorporation to the benzylpenicillin molecule or catabolism via the homogentisate pathway, which is also used to catabolize phenylalanine and tyrosine [16–21]. The first step of the phenylacetic acid catabolic pathway is a 2-hydroxylation by a microsomal cytochrome P450 monooxygenase (phenylacetate hydroxylase) encoded in *P. rubens* by the *pahA* gene (Pc21g14280) (Fig. 1). Little is known about the global responses of this microorganism to the addition of the side-chain precursor, such as specific effects on key enzymes of primary and secondary metabolism. Harris and co-workers [22] dissected the effects of phenylacetic acid on chemostat cultures using a microarray-based analysis. These authors found that the homogentisate pathway was strongly transcriptionally upregulated in those cultures supplemented with the side chain precursor, as well as those genes involved in nitrogen and sulphur metabolism. This study provided an initial global overview about the effect of phenylacetic acid on fungal physiology, although full exploitation of *P. rubens* (*P. chrysogenum*) requires the integration of knowledge from other “omics”, such as proteomics.

In this work we provide information about the catabolism of phenylacetic acid in three different strains of *P. rubens* (*P. notatum*, *P. chrysogenum* NRRL 1951 and *P. chrysogenum* Wisconsin 54–1255), characterize the function of a putative phenylacetate hydroxylase homolog in phenylacetate degradation and penicillin biosynthesis, and analyse global modifications of the *P. chrysogenum* intracellular and extracellular proteomes to the addition of the benzylpenicillin side chain precursor.

2. Materials and methods

2.1. Strains and growth conditions

Three strains of *P. rubens* (Fleming's original isolate *P. notatum*; the wild-type strain *P. chrysogenum* NRRL 1951; and the reference strain for the genome and proteome projects, *P. chrysogenum* Wisconsin 54–1255 [12, 13, 23]), were used in this work. They were grown on solid Power medium [24] for seven days at 28 °C. Conidia from one Petri dish were collected and inoculated into a 500-mL flask containing 100 mL of defined inoculation medium (DIM) with 40 g/L glucose [24]. After 24 h of incubation at 25 °C and at 250 rpm, a 10% of inoculum was added to a 500-mL flask containing 100 mL of defined production medium (MDFP), which was prepared by adding 1 g/L potassium phenylacetate, 30 g/L lactose and 10 g/L sucrose to the DIM medium without glucose, and incubated under the same conditions for different times.

For proteomics experiments, *P. rubens* (*P. chrysogenum* Wisconsin 54–1255) was grown as indicated above in defined medium with 1 g/L potassium phenylacetate. Control cultures lacked the side-chain precursor potassium phenylacetate. Cultures were incubated at 25 °C and 250 rpm and samples (mycelia and culture medium) were collected after 60 h for intracellular and extracellular proteome analysis.

For expression analysis experiments, conidia were inoculated in complex inoculum medium CIM [25] without phenylacetate. After incubation at 25 °C for 20 h in an orbital shaker (250 rpm), aliquots (5%) were inoculated in CP complex penicillin production medium [25] with 4 g/L potassium phenylacetate and incubated under the same conditions for 48 h and 60 h.

For transformation experiments, conidia were inoculated into MPPY medium (40 g/L glucose, 3 g/L $NaNO_3$, 2 g/L yeast extract, 0.5 g/L KCl, 0.5 g/L $MgSO_4{\cdot}7H_2O$, 0.01 g/L $FeSO_4{\cdot}7H_2O$, pH = 6.0) and grown for 24 h at 25 °C and 250 rpm.

2.2. Plasmid constructions for gene silencing

Plasmid pJL43-RNAi [26], which confers phleomycin resistance, was previously digested with *Nco*I and used as backbone structure for the constructions aimed to generate knock-down transformants in the Pc16g01770 gene. Oligonucleotides 1770F (5′-GATC*CCATGG*CCATGA TCCAGC-3′) and 1770R (5′-GATAG*CCATGG*CCGCCCGATC-3′), which were designed to bear *Nco*I restriction sites (in italics), were used to amplify a 473-bp exon fragment from Pc16g01770. The amplicon was digested with *Nco*I and cloned into pJL43-RNAi, thus yielding plasmid pJL43-RNAi-1770.

2.3. Transformation of P. rubens (P. chrysogenum Wisconsin 54–1255) protoplasts, extraction of genomic DNA and Southern blotting

Protoplasts were obtained and transformed as previously described [27]. Then, transformed protoplasts were grown in Czapek minimal medium (30 g/L sucrose, 2 g/L $NaNO_3$, 0.5 gLl K_2HPO_4, 0.5 g/L $MgSO_4.7H_2O$, 0.01 g/L $FeSO_4$) and further selected in Czapek minimal medium containing 30 μg/mL phleomycin.

DNA isolation and Southern blotting hybridization were carried out as previously described [28].

2.4. RNA extraction and semiquantitative RT-PCR assays

Cultures of *P. rubens* (*P. chrysogenum* Wisconsin 54–1255) were grown in complex medium as indicated above during 48 h and 60 h. Total RNA was extracted using “RNeasy Mini Kit” columns (Qiagen), following the manufacturer's instructions. Total RNA was treated with “RQ1 RNase-Free DNase” (Promega Corporation) and quantified using a NanoDrop ND-1000 spectrophotometer (Thermo Fisher Scientific).

RT-PCR was conducted with 200 ng of total RNA using the “SuperScript One-Step RT-PCR with Platinum Taq” system (Invitrogen Corporation) and applying 40 amplification cycles as recommended by the manufacturer. For the amplification of a 473-bp fragment from Pc16g01770, primers 1770F and 1770R (see above) were used. For the amplification of a 432-bp fragment from Pc22g02230, primers 2230F (5′-GGATGCTAAGGCCTATGAAGG-3′) and 2230R (5′-GAAGATCCAATG GTAAAGCCCTG-3′) were used. For the amplification of a 457-bp fragment from the *actA*-encoding β-actin gene, primers actAF (5′-CTGGCC GTGATCTGACCGACTAC-3′) and actAR (5′-GGGGGAGCGATGATCTTG ACCT-3′) were used. The absence of contaminating DNA in the RNA samples was confirmed by PCR.

For some experiments, densitometry analyses using the “Gel-Pro Analyser” software (Media Cybernetics) were performed in order to quantify the signals provided by the RT-PCR assays. The transcript levels were normalized by comparing the intensity of each mRNA signal to the β-actin mRNA signal. Expression levels were considered significantly different according to the standard deviation and when the p-

value provided by the Student's *t*-test was $p < 0.01$.

2.5. HPLC analysis

Extraction, analysis and quantitation of benzylpenicillin were carried out by HPLC using an Agilent 1100 HPLC system with an analytical 4.6 × 250 mm (5 μm) RPC18 Lichrospher® 100 column as previously described [29].

Phenylacetate and 2-hydroxyphenylacetate were extracted, analysed and quantified as follows. Culture supernatants (0.8 mL) were mixed with cold HPLC-grade methanol (1:1 ratio) and left overnight at 4 °C for protein precipitation. Then, samples were centrifuged at 13,000 rpm for 10 min at 4 °C and analysed by HPLC, which was carried out using an Agilent 1100 HPLC system with an analytical 4.6 × 150 mm (3 μm) Mediterranea Sea18 Teknokroma® column with a flow rate of 1 mL/min. Detector wavelength was set to 217 nm (for potassium phenylacetate) or 270 nm (for 2-hydroxyphenylacetate). Samples (10 μL) were injected in the HPLC using 1% trifluoroacetic acid as solvent A and acetonitrile as solvent B. The elution gradient was as follows: 10%B → 55%B linear over 15 min, 55%B → 100%B linear over 1 min, isocratic elution for 4 min, 100%B → 10%B for 0.5 min, isocratic elution for 5.5 min. Under these conditions, the retention time for potassium phenylacetate was 11.05 ± 0.15 min, whereas for 2-hydroxyphenylacetate, the retention time was 8.45 ± 0.15 min. The detection limit was 15 μg/mL.

2.6. Protein extraction

Proteins from either the mycelia (intracellular) or the culture supernatants (extracellular) were obtained as previously described [13, 23]. The final pellet was solubilized in sample buffer: 8 M urea, 2% (w/v) CHAPS, 0.5% (v/v) IPG Buffer (GE Healthcare), 20 mM DTT, 0.002% bromophenol blue. The insoluble fraction was discarded by centrifugation at 16,000 x g for 5 min. The supernatant was collected and protein concentration was determined according to the Bradford method, which showed a high reproducibility for this protein extraction protocol.

2.7. 2-DE gel electrophoresis

A solution containing 350 μg of soluble intracellular proteins or 450 μg of soluble extracellular proteins in the sample buffer (see above), was loaded onto 18-cm IPG strips (GE Healthcare), with non-linear pH 3–10 gradient (for intracellular proteins) or non-linear pH 4–7 gradient (for extracellular proteins). Focusing of proteins and equilibration of the focused IPG strips were achieved as previously described, as well as the second dimension, which was run by SDS-PAGE in 12.5% polyacrylamide in an Ettan Dalt Six apparatus (GE Healthcare) [13, 23]. Gels were dyed with Colloidal Coomassie (CC) following the "Blue Silver" staining method [30], which provides high reproducibility, as indicated before [13, 23].

2.8. Analysis of differential protein expression

Scanned 2D gels were analysed using an ImageScanner II (GE Healthcare) calibrated with a grayscale marker (Eastman Kodak Co.). Labscan 5.00 (v1.0.8) software (GE Healthcare) and the ImageMasterTM 2D Platinum v5.0 software (GE Healthcare) were used for image acquisition and analysis as previously described [13, 23]. Three biological replicates were used for each condition. After automated spot detection, spots were checked manually to eliminate any possible artefacts, such as streaks or background noise. Spot normalization, as an internal calibration to make the data independent from experimental variations among gels, was made using relative volumes (volume of each spot divided by the total volume of all the spots in the gel) to quantify and compare the gel spots. Differentially expressed proteins between two strains were considered when the ratio of the relative volume average for one specific spot (present in the three biological replicates) was higher than 1.5 or lower than −1.5 and the p-value was < 0.05.

2.9. Protein identification by MALDI-TOF MS and MS/MS

The spots of interest were manually excised from Colloidal Coomassie-stained gels by biopsy punches, placed in an Eppendorf tube, and washed twice with ddH_2O. The proteins were digested following the method of Havlis and co-workers [31] and processed for further analysis as indicated before [13, 23]. The samples were analysed with a 4800 Proteomics Analyser MALDI-TOF/TOF mass spectrometer (Applied Biosystems). A 4700 proteomics analyser calibration mixture (Cal Mix 5; Applied Biosystems) was used as external calibration. All MS spectra were internally calibrated using peptides from the trypsin digestion. The peptide mass fingerprints results, with a signal to noise (S/N) ratio > 20, were collected and represented as a list of monoisotopic molecular weights using the 4000 Series Explorer v3.5.3 software (Applied Biosystems). Well known contaminant ions (trypsin- and keratin-derived peptides) were excluded for later MS/MS analysis. Hence, the six most intensive precursors from each MS spectra with a S/N > 20 were selected for MS/MS analyses with CID (atmospheric gas was used) in 2-kV ion reflector mode and precursor mass windows of ± 7 Da. Default calibration was optimized for the MS/MS spectra.

Mascot Generic Files combining MS and MS/MS spectra were automatically created for protein identification by means of a non-redundant protein database using a local license of Mascot v 2.2 from Matrix Science through the Protein Global Server (GPS) v 3.6 (Applied Biosystems). The search parameters for peptide mass fingerprints and tandem MS spectra obtained were set as follows: (i) Uniprot Ascomycota (date 2017.07.03; 6,766,808 sequences, 3,023,177,811 residues); (ii) fixed and variable modifications were considered (Cys as S carbamidomethyl derivative and Met as oxidized methionine); (iii) one missed cleavage site was allowed; (iv) precursor tolerance was 100 ppm and MS/MS fragment tolerance was 0.3 Da; (v) peptide charge: 1 +; and (vi) the algorithm was set to use trypsin as the enzyme. Protein candidates produced by this combined peptide mass fingerprinting (PMF)/tandem MS search were considered valid when the global Mascot score was > 83 with a significance level of $p < 0.05$. Additional criteria for confident identification were that the protein match should have at least 15% sequence coverage; for lower coverages, only those proteins with at least two peptides identified were considered valid.

3. Results

3.1. Catabolism of phenylacetic acid in three different P. rubens strains

The behaviour of three different penicillin-producing strains of *P. rubens* (*P. notatum*, *P. chrysogenum* NRRL 1951 and *P. chrysogenum* Wisconsin 54–1255) was tested in the presence of phenylacetic acid. For this purpose, they were grown for 72 h in DP medium containing 1 g/L potassium phenylacetate (7 mM). All strains were able to grow in the presence of potassium phenylacetate and showed a similar growth pattern and biomass values with no significant differences along the culture time (Fig. 2A). Antibiotic production was analysed in the three strains. As expected, *P. chrysogenum* Wisconsin 54–1255 produced the highest benzylpenicillin titers (3,6 ± 1,2 mg/g dry weight at 72 h), which were 300-fold and 2000-fold higher than those provided by *P. chrysogenum* NRRL 1951 and *P. notatum*, respectively (data not shown). Phenylacetate consumption was similar in the three strains until 24 h. After this time point, *P. chrysogenum* Wisconsin 54–1255 showed a lower consumption rate than the wild-type parental strain *P. chrysogenum* NRRL 1951 and *P. notatum*, which were the only strains able to fully deplete the side chain precursor after 72 h of growth (Fig. 2B).

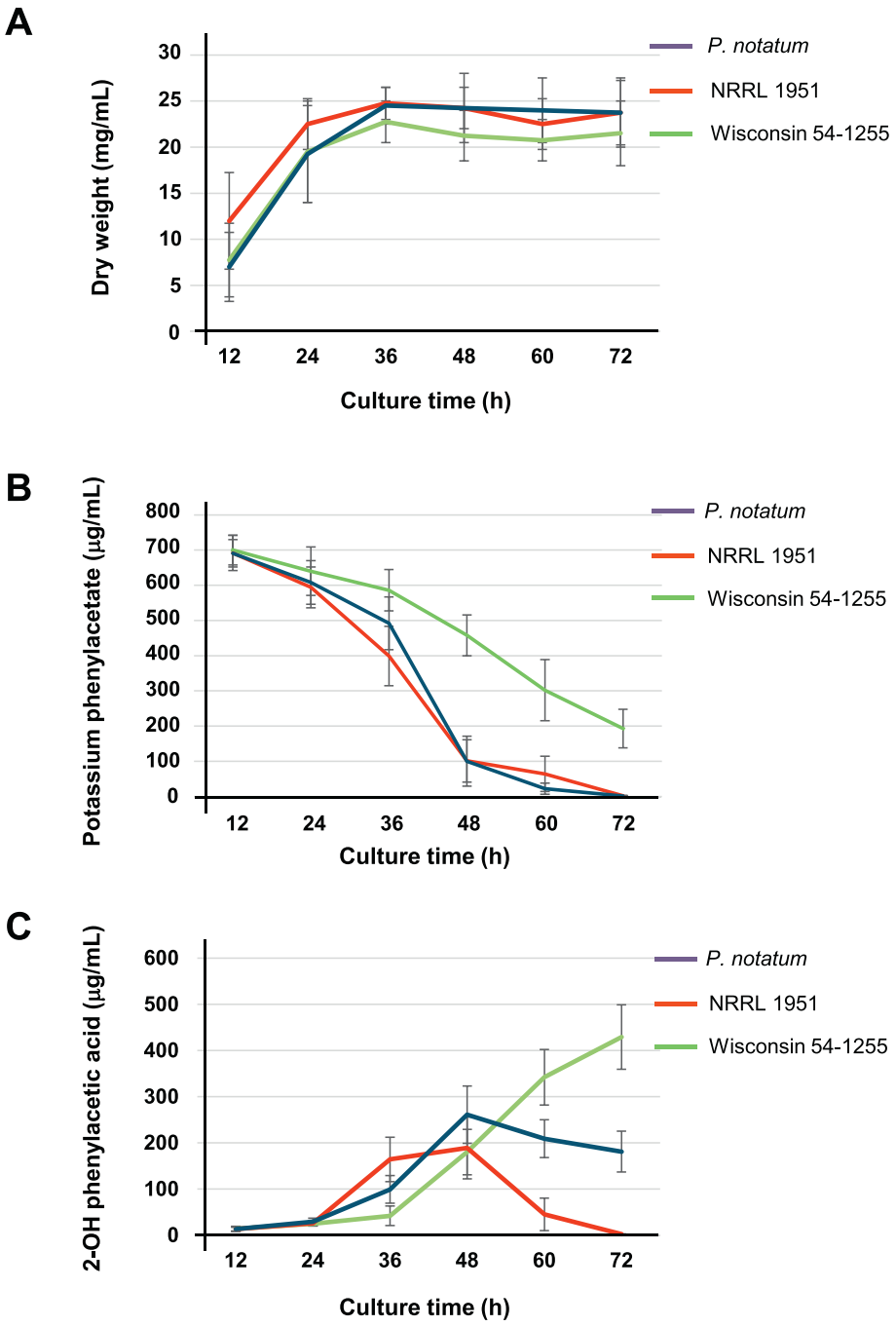

Fig. 2. Catabolism of phenylacetic acid in three strains of *P rubens* (*P. notatum*, *P chrysogenum* NRRL 1951 and *P. chrysogenum* Wis 54–1255). A) Dry weight (mg/mL) obtained from samples taken at different time points. B) Consumption of potassium phenylacetate (µg/mL) along the culture time. C) Secretion of 2-hydroxyphenylacetate (2-OH phenylacetate) (µg/mL) along the culture time. Data correspond to three biological replicates performed in triplicate.

This suggests that late steps in the catabolism of phenylacetic acid might be limiting in this strain. As a control, a parallel abiotic experiment was run with DP medium supplemented with 1 g/L potassium phenylacetate (7 mM) and subjected to similar conditions. Phenylacetate levels remained constant along the culture time, thus excluding a phenomenon of non-enzymatic degradation of this compound in the absence of *P. rubens* (data not shown). To test the phenylacetate catabolic activity of the three *P. rubens* strains, secretion of 2-hydroxyphenylacetate was assessed (Fig. 2C). Similar amounts of this metabolite were found in the culture media of these strains at early time points. *P. notatum* produced higher amounts of 2-hydroxyphenylacetate at 48 h, and a gradual decrease in the amount of this compound was observed from this time-point. *P. chrysogenum* NRRL 1951 showed a slightly different pattern, with a full depletion of this metabolite at 72 h. Interestingly, in *P. chrysogenum* Wisconsin 54–1255, 2-hydroxyphenylacetate levels in the culture medium increased from 36 h of growth until the end of the culture time (Fig. 2C).

3.2. Characterization of phenylacetate hydroxylase homologs in P. rubens (P. chrysogenum Wisconsin 54–1255)

With the aim of shedding light into the degradation of phenylacetic acid by the improved strain *P. chrysogenum* Wisconsin 54–1255, a search for *pahA*-encoded phenylacetate hydroxylase (Pc21g14280)

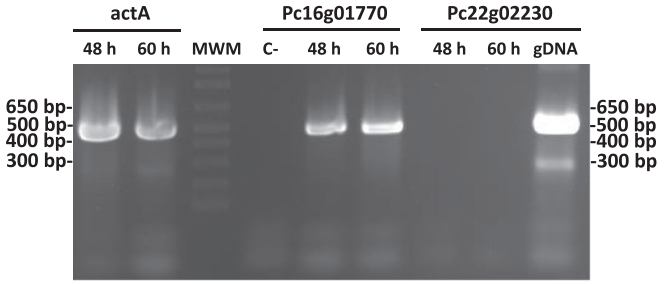

Fig. 3. Expression of putative *pahA* homologs in *P. rubens* (*P. chrysogenum* Wis 54–1255). Ethidium bromide-stained agarose gel showing the RT-PCR band (473-bp) of Pc16g01770 that has been amplified from RNA samples taken at 48 h and 60 h. The absence of contaminating DNA in the RNA samples was confirmed by PCR (C-). Note the absence of RT-PCR bands for Pc22g02230 when RNA is used and the amplification of a 432-bp PCR band from this gene when genomic DNA is used as template (gDNA). Amplification of RT-PCR fragments (457 bp) from the *actA*-encoding β-actin gene was used as a reference of transcription.

homologs was carried out in the *P. rubens* (*P. chryosogenum* Wisconsin 54–1255) genome [12]. Three proteins were found with > 50% similarity with the *pahA*-encoded protein: Pc22g02230 (65% similarity, 46% identity), Pc16g01770 (62% similarity, 44% identity) and Pc21g22560 (60% similarity, 42% identity). According to the sequence, all proteins belonged to the Cytochrome P450 superfamily. In addition, Pc21g22560 also contained GAL4-like (Zn2Cys6 binuclear cluster DNA-binding) and fungal transcription factor regulatory middle homology region domains, which suggested a different role from phenylacetate catabolism.

Therefore, we focused our research on Pc22g02230 and Pc16g01770. Expression of these genes was analysed in cultures of *P. rubens* (*P. chrysogenum* Wisconsin 54–1255), which was grown for 48 h and 60 h in complex medium in the presence of 4 g/L potassium phenylacetate. RT-PCR experiments (Fig. 3) showed that Pc16g01770 was expressed along the culture time, unlike Pc22g02230, whose transcription was not detected even after 50 amplification cycles.

According to expression data, Pc22g02230 was discarded for further analysis and the role of Pc16g01770 in phenylacetate degradation was assessed by means of gene silencing experiments. For this purpose, *P. rubens* (*P. chrysogenum* Wisconsin 54–1255) was transformed with plasmid pJL43-RNAi-1770. Integration of the silencing cassette in different transformants was confirmed by Southern blotting (Fig. 4A) after the digestion of genomic DNA with *Sph*I and *Hind*III, and hybridisation to the DIG-labelled exon fragment (the same DNA fragment that was included in the silencing cassette). All transformants and the parental strain showed the 9.4-kbp hybridisation band containing the internal Pc16g01770 gene. In addition, transformants 1, 5, 15, 38, 52 and 55 showed the 1.8-kbp band that included the silencing cassette. Attenuation of expression in these transformants was confirmed by RT-PCR (Fig. 4B). All transformants, except 52 and 55, showed significant ($p < 0.05$) reduced expression (ranging from 42% in transformant 15 to 17% in transformant 38) of the Pc16g01770 gene, and were phenotypically characterized.

Cultures of *P. chrysogenum* Wisconsin 54–1255 and knock-down transformants 1, 5, 15 and 38 were conducted in defined medium in the presence of 1 g/L potassium phenylacetate. Samples were collected at 24 h, 48 h and 72 h and the presence of non-consumed phenylacetic acid, 2-hydroxyphenylacetic acid and benzylpenicillin in the culture supernatants was analysed by HPLC. Transformants 1, 5 and 15 showed a slight (up to 20%) significant ($p < 0.05$) increase in the phenylacetic acid levels at 72 h regarding the values provided by the parental Wisconsin 54–1255 strain (Fig. 5A). Also, the presence of 2-hydroxyphenylacetic acid was assessed in those transformants. In general, they showed significant ($p < 0.05$) slightly reduced levels (up to 25%) of this compound at 48 h and 72 h (transformant 5 did not provide a significant decrease at 72 h), in comparison with the values provided by the parental strain (Fig. 5B). This behaviour may be due to a reduced degradation of the benzylpenicillin side chain precursor in the knock-down transformants. Benzylpenicillin specific production remained similar between transformants and the parental Wisconsin 54–1255 strains (Fig. 5C). These results suggest that Pc16g01770 may have a residual activity in phenylacetic acid degradation in the Wisconsin 54–1255 strain, this catabolic activity having no effect on benzylpenicillin biosynthesis (see Discussion).

3.3. Effect of phenylacetic acid on the intracellular and extracellular proteomes of *P. rubens* (*P. chrysogenum* Wisconsin 54–1255)

In order to get more insight into the metabolic processes modified by the presence of the benzylpenicillin side chain precursor, a proteome-wide analysis was carried out in *P. rubens* (*P. chrysogenum* Wisconsin 54–1255).

For this purpose, cultures were conducted with this fungal strain in the presence and absence of 1 g/L phenylacetic acid. Samples included both mycelia (for intracellular proteome analysis) and culture supernatants (for extracellular proteome analysis) and were taken at 60 h of growth. Protein fractions were analysed by 2-DE and tandem MS spectrometry.

3.3.1. Intracellular proteome

The 2-DE gels with the intracellular protein fractions obtained from both conditions were compared to each other (Fig. 6). A total of 22 spots (D1-D22 including 23 proteins) resulted overrepresented, whereas 53 spots (C1-C53 including 56 proteins) were underrepresented after phenylacetic acid addition (Supplementary Tables S1 and S2). Functions were inferred for these proteins (Tables 1 and 2) and the main findings are summarized below.

Only one protein from the homogentisate pathway was found overrepresented after the addition of phenylacetic acid (Table 1). Spot D6 (4.5-fold overrepresented) contains the fumaryl acetoacetase (Pc12g09030), which is involved in the last step of the catabolic pathway of phenylacetic acid (see Discussion).

Interestingly, several proteins related to penicillin biosynthesis were also found overrepresented after the addition of the benzylpenicillin side chain precursor. The first one is IAT (Pc21g21370), one of the penicillin biosynthetic enzymes, which is included in spot D11 (5.8-fold overrepresented). Other important proteins are present in Spot D4 (2.4-fold overrepresented in the presence of phenylacetic acid and including a hypothetical cystathionine beta synthase) Spot D23 (only detected with phenylacetic acid and including a probable ketol-acid reductoisomerase ilv-2) and Spot D22 (only detected after supplementation with phenylacetic acid and containing a probable thioredoxin peroxidase (Pc22g04430)). Another interesting protein that resulted overrepresented after phenylacetic acid addition is S-adenosylmethionine synthase, which is included in spot D14 (2.9-fold overrepresented) (See Discussion).

Several proteins that are underrepresented due to the presence of phenylacetic acid (Table 2) belong to the glycolysis and tricarboxylic acid cycle. Examples are provided by spots C7 (Pc18g01220, probable fructose-bisphosphate aldolase), C12 (Pc18g06000, probable pyruvate kinase), C27 and C28 (both including Pc20g01610, a probable mitochondrial malate dehydrogenase), C40 (Pc22g02000, a probable mitochondrial aconitate hydratase), and C45 and C46 (both including Pc12g06870, a probable alpha subunit of succinyl coenzyme A synthase). In addition, three spots related to the metabolism of acetyl-CoA were also found underrepresented under these conditions: spot C9 (Pc21g20480, probable ATC citrate lyase), spot C11 (Pc12g03130, a probable acetyl-CoA hydrolase) and spot C44 (Pc22g11710, probable alpha subunit E1 of the pyruvate dehydrogenase complex). Related to this finding is the fact that spot C2, which includes a probable *N*-

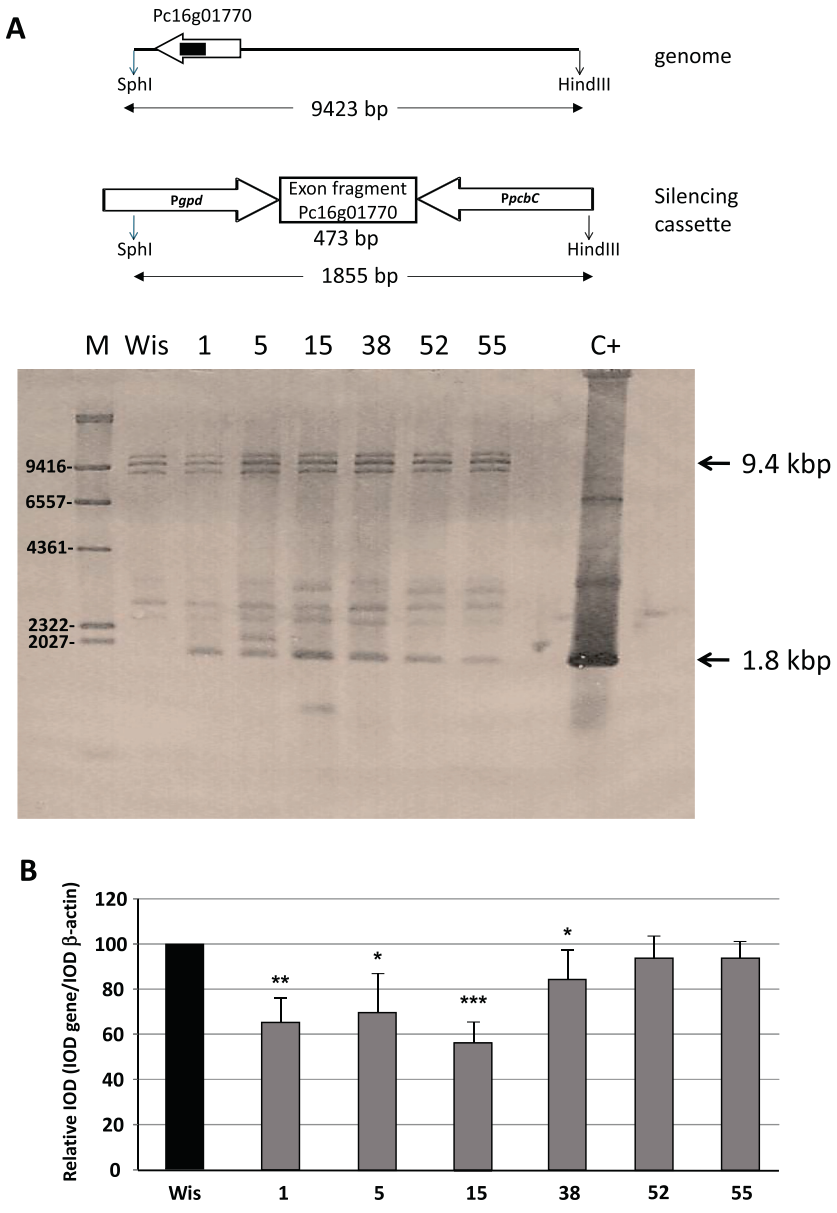

Fig. 4. Gene silencing of Pc16g01770. A) Southern blot analysis of different transformants (1, 5, 15, 38, 52 and 55) and the parental *P. rubens* (*P. chrysogenum* Wisconsin 54–1255 strain) (Wis). The 473-bp exon fragment (indicated as a black box inside the corresponding gene) included in the silencing cassette, was used as probe. All transformants show the 1855-bp hybridisation band corresponding to the silencing cassette. Note the presence of the 9423-bp genomic band containing the endogenous Pc16g01770 gene. Additional hybridisation bands are likely due to partial digestion of genomic DNA. B) Relative expression (quantified by RT-PCR) of Pc16g01770 in different transformants compared to the Wisconsin 54–1255 strain (Wis; reference value set to 100). Values correspond to the mean plus standard deviation of three independent experiments. Statistical significance by ANOVA test is represented above error bars as "*" ($0.01 \leq P < 0.05$); "**" ($0.001 \leq P < 0.01$); "***" ($P < 0.001$).

acetylglucosamine-6-phosphate deacetylase (Pc22g10010), is 5.28-fold underrepresented in the presence of phenylacetic acid. This enzyme deacetylates amino sugars to yield glucosamine-6-phosphate and acetate.

Another interesting group of proteins that resulted underrepresented after the addition of the benzylpenicillin side chain precursor were related to protein folding, modification or degradation. This is the case of spots C5 (Pc22g11240, probable heat shock protein 70 hsp70), C8 (Pc22g19990, probable endonuclease *Sce*I 75 kDa subunit Ens1 with putative hsp70 activity), C21 and C41 (both including Pc22g10220, a probable dnaK-type molecular chaperone), C29 (Pc21g16970, vacuolar serine proteinase AAG44693 or allergen Pen n 18), C33 (probable proteasome component PRE6), C36 (Pc22g13950, probable vacuolar aminopeptidase Ysci) and C49 (Pc20g09400, probable dipeptidyl-peptidase V).

A subset of proteins related to oxidative stress response was also underrepresented in the presence of phenylacetic acid. Examples are provided by spots C3 (Pc12g14620, probable flavohemoglobin Fhp), C16 and C17 (both including Pc16g13280, a probable glutathione reductase), C30 (Pc16g09250, probable cytochrome-b5 reductase) and C48 (Pc18g00790, probable glutathione S-transferase).

3.3.2. *Extracellular proteome*

The 2-DE gels including the extracellular protein fractions obtained in the presence and absence of phenylacetic acid were also compared to each other (Fig. 7). A total of 45 spots, named P1-P45 and including 49 proteins (36 different proteins), resulted overrepresented, whereas 14 spots, named S1-S14 and including 16 proteins (12 different proteins), were underrepresented after phenylacetic acid addition (Supplementary Tables S3 and S4). Secretion of those proteins due to the presence of classical signal peptides or through a non-classical secretory mechanism was predicted as indicated in our previous work [23]. A total of 38 different proteins out of the 48 proteins found differentially represented in the secretome were predicted to contain either classical or non-classical signal sequences (Tables 3 and 4) (see Discussion). Functions were inferred for these proteins and the main findings are summarized below.

The most important extracellular protein overrepresented after the addition of phenylacetic acid is included in spot P16. This spot is only detected under these conditions and contains the glutamate dehydrogenase (encoded by the *gdhA* gene), which lacks classical or non-classical signal sequences for secretion (see Discussion).

Some proteins from the glycolysis, tricarboxylic acid cycle and

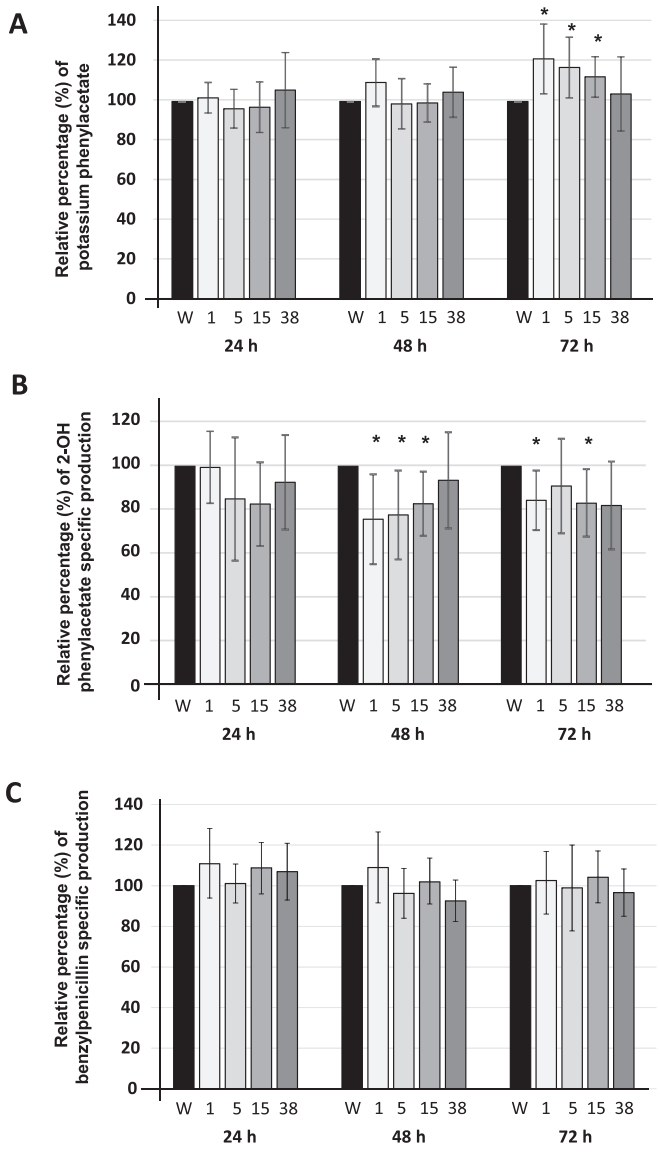

Fig. 5. Relative percentage (%) of A) potassium phenylacetate, B) 2-hydroxyphenylacetate (2-OH phenylacetate) specific production and B) benzylpenicillin specific production assessed in samples obtained at 24 h, 48 h and 72 h from cultures of *P. rubens* (*P. chrysogenum* Wisconsin 54–1255) (W) and different Pc16g01770 knock-down transformants (1, 5, 15 and 38). Results are represented as the mean ± standard deviation from three independent experiments carried out in triplicate. Values were normalized to those provided by the Wisconsin 54–1255 strain (W) at each time-point, which were set to 100%. Statistical significance by ANOVA test is represented above error bars as "*" ($0.01 \leq P < 0.05$).

pentose phosphate pathways are also overrepresented under these conditions, including a probable mitochondrial aconitate hydratase Aco1 (Pc22g02000, spots P4, P5 and P9), an enolase (Pc14g01740, spots P18 and P43), and a probable transaldolase Tal1 (Pc21g16950, spot P26). Interestingly, none of these proteins are predicted to be secreted (Table 3) (see Discussion).

All proteins underrepresented in the presence of the benzylpenicillin side chain precursor are predicted to be secreted (Table 4). Most of them are involved in plant cell wall and plant tissues degradation. This is the case of spots S3 and S11 (both including Pc22g20290, a probable polygalacturonase pgaI), S5 (Pc22g24890, probable pectate lyase plyA, and Pc20g07020, endo-1,4-beta-xylanase A precursor XylP), S11 (Pc22g20290, probable polygalacturonase pgaI), S12 and S13 (both including Pc20g07030, a probable 1,4-beta-Δ-arabinoxylan arabinofuranohydrolase axhA).

The presence of phenylacetic acid downregulates the synthesis of a probable cephalosporin esterase (Pc12g13400). This wide substrate spectrum esterase forms deacetylcephalosporin C and acetate using cephalosporin C as substrate and is included in spot S6 (5.2-fold underrepresented under these conditions).

4. Discussion

One of the most important milestones in the history of penicillins is the finding that addition of specific side chain precursors (e.g. phenylacetic acid) to culture media, directed the biosynthetic process mainly towards benzylpenicillin (penicillin G) [32], which is the main biosynthetic penicillin produced under industrial conditions. Distinct *P. rubens* strains behave in a different way regarding detoxification of phenylacetic acid. Unlike *P. notatum*, *P. chrysogenum* is unable to grow on phenylacetic acid as sole carbon source, although it can efficiently oxidize it, hence suggesting a block in the catabolic pathway to fumarate and acetoacetate [14, 15]. These authors reported that modifications (L181F and A394V) in the phenylacetate hydroxylase (the first enzyme of the catabolic pathway of phenylacetic acid) during strain improvement programs gave rise to loss-of-functions mutations, thus leading to reduced degradation of phenylacetic acid and to penicillin overproduction in *P. chrysogenum* [14, 15]. Our results (Fig. 2) indicate that in the presence of sucrose and lactose as carbon sources, *P. chrysogenum* is able not only to incorporate phenylacetic acid to the benzylpenicillin biosynthetic pathway, but also to convert it to 2-hydroxyphenylacetic acid by the phenylacetate hydroxylase via the homogentisate pathway. In addition, *P. chrysogenum* Wisconsin 54–1255 showed an increase in 2-hydroxyphenylacetate levels along the culture time in comparison with *P. notatum* and *P. chrysogenum* NRRL 1951, which accumulate lower amounts of this compound likely due to a faster metabolization to 2, 5-dihydroxyphenylacetate at late time points. This phenomenon is similar to that reported in *P. chrysogenum* overproducing strains, where significant amounts of 2-hydroxyphenylacetic acid are detected in the fermentation broth [15]. Therefore, both detoxification mechanisms seem to coexist in different species of *P. rubens*, but with different efficiencies. While catabolic detoxification is more efficient in *P. notatum* and *P. chrysogenum* NRRL 1951 than in *P. chrysogenum* Wisconsin 54–1255, detoxification by means of penicillin formation is more efficient in *P. chrysogenum* Wisconsin 54–1255 than in the other two strains. The fact that *P. chrysogenum* Wisconsin 54–1255 shows catabolic detoxification suggests a partial blockage of phenylacetate hydroxylase activity in improved strains of *P. chrysogenum*, or the presence of at least another protein with phenylacetate hydroxylase activity in this microorganism. This question can be elucidated by comparison to the information published for *A. nidulans*, another penicillin-producing fungus.

A. nidulans, known to degrade efficiently phenylacetic acid by different enzymes, is also able to utilize phenylacetate as a carbon source via homogentisate, phenylacetic acid being converted to 2-hydroxyphenylacetate by means of a 2-hydroxylation reaction catalysed by a cytochrome P450 monooxygenase, which is encoded by the *phacA* gene [18]. In addition, the existence of another cytochrome P450 monooxygenase (encoded by the *phacB*) with 3-hydroxyphenylacetate 6-hydroxylase and 3,4-dihydroxyphenylacetate 6-hydroxylase activities that forms 2,5-dihydroxyphenylacetate (homogentisate) and can also convert phenylacetic acid into 2-hydroxyphenylacetate, has been reported in this microorganism [20]. Interestingly, we found three proteins (Pc22g02230, Pc16g01770 and Pc21g22560) from the cytochrome P450 superfamily that show > 50% similarity with the *pahA*-encoded protein (Pc21g14280) in the *P. rubens* (*P. chrysogenum* Wisconsin 54–1255) genome. Unlike Pc22g02230, Pc16g01770 was expressed under the conditions tested (Fig. 3). This result is consistent with previous transcriptomics data, which reported high transcription rate of

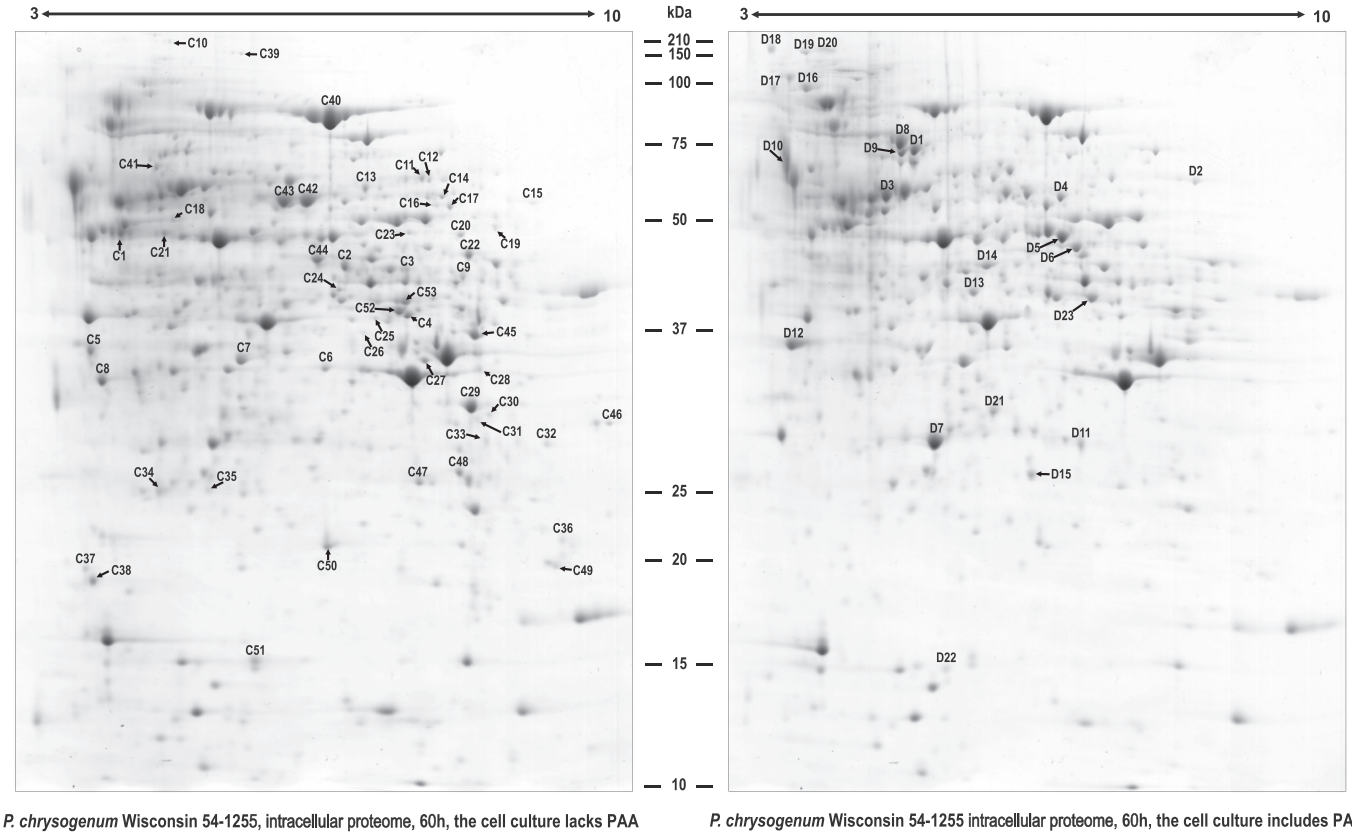

Fig. 6. Effect of phenylacetic acid (PAA) in the intracellular proteome of *P. rubens* (*P. chrysogenum* Wisconsin 54–1255). Intracellular proteins obtained from mycelia of *P. rubens* (*P. chrysogenum* Wisconsin 54–1255) grown for 60 h in DP medium with and without 1 g/L potassium phenylacetate, were separated by 2-DE using 18-cm wide-range IPG strips (pH 3–10 NL) and 12.5% SDS-PAGE gels, which were stained with CC following the "Blue Silver" staining method. Those spots overrepresented without PAA (underrepresented with PAA) are designated as "C", whereas the letter "D" was used to designate those spots overrepresented in the presence of PAA. The spots differentially represented in each condition are numbered and correspond to those proteins listed in Tables 1 ("D" spots) and 2 ("C" spots) and Supplementary Tables S1 ("D" spots) and S2 ("C" spots).

Pc16g01770 and transcriptional induction in the presence of phenylacetate. However, Pc21g22560 and Pc22g02230 exhibited null expression levels and no transcriptional induction under the same conditions in chemostat cultivations [12]. The protein encoded by Pc16g01770 shows 90% similarity and 82% identity with the *A. nidulans phacB*-encoded cytochrome P450 monooxygenase, suggesting a possible role of this protein in the formation of 2,5-dihydroxyphenylacetate (homogentisate) and in phenylacetate hydroxylation. The latter was tested by gene knock-down experiments, where most of the transformants silenced in the expression of Pc16g01770 showed a slight decrease in 2-hydroxyphenylacetate levels (Fig. 5). These results point to the presence of at least one additional enzyme, encoded by Pc16g01770, with residual phenylacetate hydroxylase activity in *P. chrysogenum* Wisconsin 54–1255. However, additional experiments (e.g. heterologous expression, biochemical characterization and analysis of substrate specificity) are still required to confirm the role played by the protein encoded by Pc16g01770 in the homogentisate pathway.

Interestingly, Pc16g01770 and the *pahA*-encoded phenylacetate hydroxylase lack a canonical PTS1 signal, which is a target sequence present at the C terminus that allows import of proteins into peroxisomes [33, 34]. Therefore, phenylacetate degradation via the homogentisate pathway by the protein encoded by Pc16g01770 and the *pahA*-encoded phenylacetate hydroxylase likely takes place during its way to the peroxisomal matrix. The transport of phenylacetic acid from the culture medium to the cytoplasm and then to peroxisomes has been a matter of discrepancy. Either active transport [35, 36] or passive diffusion [37], have been suggested as mechanisms for internalization of the benzylpenicillin side-chain precursor. More recently, a process of two consecutive steps (facilitated diffusion in the plasma membrane and active transport in the peroxisomal membrane) has been suggested after the characterization of a MFS transporter (PaaT) that participates in the translocation of phenylacetic acid from the cytosol to the peroxisomal lumen across the peroxisomal membrane of *P. rubens* [38]. Once phenylacetic acid is present within peroxisomes, it is activated by aryl-CoA ligases and incorporated into the penicillin biosynthetic pathway. The percentage of phenylacetic acid being incorporated into either of these two pathways (i.e. catabolism via homogentisate and benzylpenicillin biosynthesis) seems to be highly dependent on the strain, as previously suggested [14, 15].

Phenylacetic acid has a clear direct involvement in benzylpenicillin biosynthesis due to its participation as side chain precursor. In an attempt to characterize other roles that this molecule can play regarding penicillin production, we decided to carry out a global comparative proteomics analysis in *P. rubens* (*P. chrysogenum* Wisconsin 54–1255) with and without phenylacetic acid addition. Unexpectedly, only one protein (fumaryl acetoacetase; Pc12g09030) involved in the catabolism of the side chain precursor was induced by phenylacetate. Previous transcriptomics analysis reported that all genes of the homogentisate pathway for phenylacetate catabolism were strongly upregulated in the presence of phenylacetic acid [22]. These authors used a high-producing *P. chrysogenum* strain grown under glucose-limited chemostat conditions, which may be one of the main reasons for the upregulation of the whole catabolic pathway.

Among the intracellular proteins whose synthesis was induced in the presence of this side chain precursors, there are several enzymes related to β-lactam biosynthesis. The most important one is IAT

Table 1
Intracellular proteins overrepresented at 60 h in the presence of phenylacetic acid. Fold increase and p-value are indicated. Proteins that are only detected after the addition of phenylacetic acid are denoted as N/A.

Spot	ORF	Accession No	Similarity	Fold change	P-Value	Function
D1	Pc22g10220	gi|211592047	strong similarity to dnaK-type molecular chaperone Ssb2 - *Saccharomyces cerevisiae*	4.7	3.20E-03	Protein fate. Protein folding, modification and destination
D2	Pc18g05320	gi|211587092	strong similarity to IMP dehydrogenase IMH3 -*Candida albicans*	3.1	1.64E-04	GTP biosynthesis
D3	Pc12g16040	gi|211583021	strong similarity to phosphoglycerate mutase pgm - *Bacillus subtilis*	3.1	1.73E-03	Glycolysis
D4	Pc13g05320	gi|211583586	strong similarity to hypothetical cystathione beta-synthase cysB - *Dictyostelium discoideum*	2.4	4.13E-05	Amino Acid Metabolism
D5	Pc16g04730	gi|211585447	phosphoglycerate kinase pgkA-*Penicillium chrysogenum*	20.2	7.70E-06	Glycolysis
D6	Pc12g09030	gi|211582350	strong similarity to fumarylacetoacetase -*Homo sapiens*	4.5	2.48E-03	Homogentisate pathway
D7	Pc12g00830	gi|211581603	strong similarity to sorbitol utilization protein sou2 - *Candida albicans*	2.7	1.83E-05	Carbohydrate Metabolism. (Related to short-chain alcohol dehydrogenases)
D8	Pc22g19990	gi|211592918	strong similarity to endonuclease SceI 75 kDa subunit Ens1 - *Saccharomyces cerevisiae*	N/A	N/A	Protein fate. Protein folding, modification and destination. (Putative function as hsp70)
D9	Pc22g10220	gi|211592047	strong similarity to dnaK-type molecular chaperone Ssb2 - *Saccharomyces cerevisiae*	3	4.76E-03	Protein fate. Protein folding, modification and destination
D10	Pc21g16870	gi|211590398	strong similarity to hypothetical protein smik_17056 - *Saccharomyces mikatae*	N/A	N/A	Unknown
D11	Pc21g21370	gi|211590823	acyl-coenzyme A:isopenicillin N acyltransferase (acyltransferase) AAT/PenDE-*Penicillium chrysogenum*	5.8	2.80E-05	Penicillin biosynthesis
D12	Pc13g08810	gi|211583926	strong similarity to elongation factor 1beta EF-1 - *Oryctolagus cuniculus*	5.8	1.19E-05	Translation
	Pc20g13270	gi|211588542	strong similarity to nascent polypeptide-associated complex alpha chain alpha-NAC - *Mus musculus*	5.8	1.19E-05	Protein fate. Protein folding, modification and destination
D13	Pc22g05790	gi|211591628	strong similarity to transcription activator Adr1 - *Saccharomyces cerevisiae*	2.6	2.95E-03	Transcription
D14	Pc16g04380	gi|211585413	strong similarity to S-adenosylmethionine synthetase eth-1 - *Neurospora crassa*	2.9	2.93E-02	Methionine cycle
D15	Pc22g06690	gi|211591714	weak similarity to versicolorin reductase verA - *Aspergillus nidulans*	4.8	6.22E-05	Redox metabolism
D16	Pc21g19270	gi|211590629	strong similarity to valosin-containing protein like AAA-ATPase Cdc48 - *Saccharomyces cerevisiae*	N/A	N/A	Protein fate. Protein folding, modification and destination
D17	Pc22g12670	gi|211592227	strong similarity to hypothetical protein contig_1_67_scaffold_4.tfa_440wg - *Aspergillus nidulans*	N/A	N/A	Unknown
D18	Pc22g05690	gi|211591618	strong similarity to hypothetical protein contig12.tfa_1730cg - *Aspergillus fumigatus*	N/A	N/A	Unknown
D19	Pc12g11270	gi|211582564	strong similarity to hypothetical protein contig1492_0.tfa_1860cg - *Aspergillus fumigatus*	N/A	N/A	Unknown
D20	Pc22g05690	gi|211591618	strong similarity to hypothetical protein contig12.tfa_1730cg - *Aspergillus fumigatus*	N/A	N/A	Unknown
D21	Pc21g12310	gi|211589973	hypothetical protein [*Penicillium chrysogenum*]	2.4	5.31E-03	Unknown
D22	Pc22g04430	gi|211591498	strong similarity to thioredoxin peroxidase like protein An06g01660 - *Aspergillus niger*	N/A	N/A	Oxidative stress response

Table 2
Intracellular proteins underrepresented at 60 h in the presence of phenylacetic acid. Fold decrease and p-value are indicated. Proteins that are not detected after the addition of phenylacetic acid are denoted as N/A.

Spot	ORF	Accession No	Similarity	Fold change	P-Value	Function
C1	Pc22g22810	gi|211593192	strong similarity to sulphydryl oxidase Sox from patent EP565172-A1 - *Aspergillus niger*	−3.3	1.1E-02	Oxidation of sulfhydryl compounds
C2	Pc22g10010	gi|211592027	strong similarity to *N*-acetylglucosamine-6-phosphate deacetylase CaNAG2 -*Candida albicans*	−5.3	2.9E-05	Aminosugars metabolism
C3	Pc22g10140	gi|211592039	strong similarity to cytosolic acetyl-CoA *C*-acetyltransferase Erg10 - *Saccharomyces cerevisiae*	−4.8	8.3E-04	Mevalonate metabolism (isoprenoids biosynthesis)
	Pc12g14620	gi|211582885	strong similarity to flavohemoglobin Fhp -*Alcaligenes eutrophus*	−4.8	8.3E-04	Oxidative stress response
C4	Pc20g15580	gi|211588765	strong similarity to NADPH-dependent aldehyde reductase - *Sporobolomyces salmonicolor*	−2.2	2.1E-03	Reduction of a variety of aldehydes and carbonyls. Detoxification of aldehyde inhibitors
C5	Pc22g11240	gi|211592088	strong similarity to heat shock protein 70 hsp70 - *Ajellomyces capsulatus*	−4.7	1.6E-02	Protein fate. Protein folding, modification and destination
C6	Pc12g12040	gi|211582639	strong similarity to translation elongation factor eEF-2 - *Cricetulus griseus*	−4.7	3.8E-03	Translation
C7	Pc18g01220	gi|211586700	strong similarity to fructose-bisphosphate aldolase Fba1 - *Saccharomyces cerevisiae*	−4.6	2.1E-05	Glycolysis
C8	Pc22g19990	gi|211592918	strong similarity to endonuclease SceI 75 kDa subunit Ens1 - *Saccharomyces cerevisiae*	−7.6	1.5E-03	Protein fate. Protein folding, modification and destination. (Putative function as hsp70)
C9	Pc21g20480	gi|211590746	strong similarity to ATP citrate lyase ACL1 -*Sordaria macrospora*	N/A	N/A	Acetyl-CoA metabolism. Carbohydrate and lipids metabolism
C10	Pc16g06130	gi|211585572	strong similarity to alpha-glucan synthase mok1p -*Schizosaccharomyces pombe*	N/A	N/A	Cell wall and morphogenesis
C11	Pc12g03130	gi|211581818	strong similarity to acetyl-CoA hydrolase Ach1 - *Saccharomyces cerevisiae*	N/A	N/A	Acetyl-CoA metabolism. Acetate utilization
C12	Pc18g06000	gi|211587160	strong similarity to pyruvate kinase pkiA -*Aspergillus niger*	N/A	N/A	Glycolysis
C13	Pc18g00980	gi|211586677	strong similarity to hypothetical trunk lateral cell specific gene HrTLC1 - *Halocynthia roretzi*	N/A	N/A	Redox metabolism
C14	Pc21g02360	gi|211589011	strong similarity to GU4 nucleic-binding protein 1 Arc1 - *Saccharomyces cerevisiae*	N/A	N/A	Protein with binding function or cofactor requirement. Binds to tRNA and functions as a cofactor for the methionyl-tRNA synthetase (MetRS) and glutamyl-tRNA synthetase (GluRS)
C15	Pc12g03370	gi|211581841	strong similarity to mitochondrial F1-ATPase alpha-subunit Atp1 - *Saccharomyces cerevisiae*	N/A	N/A	Protein transport inside mitochondria
C16	Pc16g13280	gi|211586250	strong similarity to glutathione reductase Glr1 - *Saccharomyces cerevisiae*	N/A	N/A	Oxidative stress response
C17	Pc16g13280	gi|211586250	strong similarity to glutathione reductase Glr1 - *Saccharomyces cerevisiae*	N/A	N/A	Oxidative stress response
C18	Pc13g13470	gi|211584381	strong similarity to tubulin beta chain beta-tubulin like protein An08g03190 - *Aspergillus niger*	N/A	N/A	Cellular structure
C19	Pc16g11790	gi|211586103	strong similarity to fructosyl amine oxygen oxidoreductase - *Aspergillus fumigatus*	N/A	N/A	Oxidative deglycation of Amadori products (glycated low molecular weight amino acids) to yield amino acids, glucosone and H2O2
C20	Pc16g07470	gi|211585695	strong similarity to glycine decarboxylase subunit T Gcv1 - *Saccharomyces cerevisiae*	N/A	N/A	Aminoacid metabolism. Catabolism of glycine to 5,10-methylene-THF
C21	Pc22g10220	gi|211592047	strong similarity to dnaK-type molecular chaperone Ssb2 - *Saccharomyces cerevisiae*	N/A	N/A	Protein fate. Protein folding, modification and destination
C22	Pc20g02910	gi|211587580	strong similarity to aspartate-semialdehyde dehydrogenase Hom2 - *Saccharomyces cerevisiae*	N/A	N/A	Aminoacid metabolism
C23	Pc22g08080	gi|211591841	strong similarity to actin interacting protein like protein An02g14620 - *Aspergillus niger*	N/A	N/A	Cellular structure
C24	Pc20g04810	gi|211587757	strong similarity to estrogen receptor-binding cyclophilin cypD - *Bos primigenius taurus*	N/A	N/A	Protein with binding function or cofactor requirement
C25	Pc18g02290	gi|211586806	strong similarity to 2-nitropropane dioxygenase precursor ncd-2 - *Neurospora crassa*	N/A	N/A	Oxidation of nitroalkanes into their corresponding carbonyl compounds and nitrite
C26	Pc13g10770	gi|211584117	strong similarity to cAMP-dependent protein kinase regulatory subunit pkaR - *Aspergillus niger*	N/A	N/A	Protein fate. Protein phosphorylation
C27	Pc20g01610	gi|211587455	strong similarity to mitochondrial malate dehydrogenase Mdh1 - *Saccharomyces cerevisiae*	N/A	N/A	Citric acid cycle

(*continued on next page*)

Table 2 (*continued*)

Spot	ORF	Accession No	Similarity	Fold change	P-Value	Function
C28	Pc20g01610	gi|211587455	strong similarity to mitochondrial malate dehydrogenase Mdh1 - *Saccharomyces cerevisiae*	N/A	N/A	Citric acid cycle
	Pc14g02010	gi|211584816	strong similarity to hypothetical protein contig_1_98_scaffold_6.tfa_1090cg - *Aspergillus nidulans*	N/A	N/A	Unknown
C29	Pc21g16970	gi|255955889	vacuolar serine proteinase AAG44693-*Penicillium chrysogenum*. Allergen Pen n 18 [*Penicillium chrysogenum*]	N/A	N/A	Protein fate. Protein folding, modification and destination
C30	Pc16g09250	gi|211585866	strong similarity to cytochrome-b5 reductase Mcr1 - *Saccharomyces cerevisiae*	N/A	N/A	Oxidative stress response
C31	Pc12g01420	gi|211581659	strong similarity to riboflavin biosynthesis protein Rib7 - *Saccharomyces cerevisiae*	N/A	N/A	Cofactor biosynthesis
C32	Pc12g16540	gi|211583071	strong similarity to cytosolic aspartate–tRNA ligase Dps1 - *Saccharomyces cerevisiae*	N/A	N/A	aminoacyl-trna biosynthesis
C33	proteasome component PRE6 [*Aspergillus terreus* NIH2624]	gi|115437366	proteasome component PRE6 [*Aspergillus terreus* NIH2624]	N/A	N/A	Protein fate. Protein folding, modification and destination
C34	Pc20g11850	gi|211588406	strong similarity to elongation factor 1-gamma 1 Tef3 - *Saccharomyces cerevisiae*	N/A	N/A	Translation
C35	Pc20g03290	gi|211587616	strong similarity to hypothetical protein contig1495_2.tfa_640cg - *Aspergillus fumigatus*	N/A	N/A	Unknown
C36	Pc22g13950	gi|211592336	strong similarity to vacuolar aminopeptidase Ysci -*Saccharomyces cerevisiae*	N/A	N/A	Protein fate. Protein folding, modification and destination
C37	Pc21g03140	gi|211589089	strong similarity to cell cycle regulator p21 protein wos2p - *Schizosaccharomyces pombe*	N/A	N/A	Cell cycle and DNA processing
C38	Pc21g03140	gi|211589089	strong similarity to cell cycle regulator p21 protein wos2p - *Schizosaccharomyces pombe*	N/A	N/A	Cell cycle and DNA processing
C39	Pc06g00710	gi|211581297	strong similarity to 150 kDa oxygen regulated protein ORP150 - *Rattus norvegicus*	N/A	N/A	Unknown
C40	Pc22g02000	gi|211591261	strong similarity to mitochondrial aconitate hydratase Aco1 - *Saccharomyces cerevisiae*	−1.2	1.3E-03	Citric acid cycle
C41	Pc22g10220	gi|211592047	strong similarity to dnaK-type molecular chaperone Ssb2 - *Saccharomyces cerevisiae*	−1.7	9.6E-02	Protein fate. Protein folding, modification and destination
C42	Pc18g00980	gi|211586677	strong similarity to hypothetical trunk lateral cell specific gene HrTLC1 - *Halocynthia roretzi*	−2.5	1.8E-03	Redox metabolism
C43	Pc18g00980	gi|211586677	strong similarity to hypothetical trunk lateral cell specific gene HrTLC1 - *Halocynthia roretzi*	−2.0	1.0E-03	Redox metabolism
C44	Pc22g11710	gi|211592134	strong similarity to alpha subunit E1 of the pyruvate dehydrogenase complex Pda1 - *Saccharomyces cerevisiae*	−2.9	7.9E-03	Biosynthesis of acetyl CoA from pyruvate
C45	Pc12g06870	gi|211582144	strong similarity to succinyl coenzyme A synthase alpha subunit SYRTSA - *Rattus norvegicus*	−1.8	2.2E-03	Citric acid cycle
C46	Pc12g06870	gi|211582144	strong similarity to succinyl coenzyme A synthase alpha subunit SYRTSA - *Rattus norvegicus*	N/A	N/A	Citric acid cycle
	Pc22g17950	gi|211592721	strong similarity to hypothetical protein contig40.tfa_680wg - *Aspergillus fumigatus*	N/A	N/A	Unknown
C47	Pc22g01260	gi|211591187	strong similarity to small G-protein Gsp1 -*Candida albicans*	−1.6	1.6E-02	Cellular communication/Signal transduction mechanism
C48	Pc18g00790	gi|211586658	strong similarity to glutathione S-transferase like protein An02g06560 - *Aspergillus niger*	−2.9	6.2E-03	Oxidative stress response
C49	Pc20g09400	gi|211588171	strong similarity to dipeptidyl-peptidase V DPP V - *Aspergillus fumigatus*	−7.8	2.0E-03	Protein fate. Protein folding, modification and destination
C50	Pc22g25220	gi|211593426	strong similarity to 1,4-benzoquinone reductase qr. - *Phanerochaete chrysosporium*	−1.9	1.1E-03	Reduction of methoxylated, lignin-derived quinones
C51	Pc22g09580	gi|211591986	strong similarity to acid phosphatase aphA -*Aspergillus ficuum*	−2.3	6.2E-05	Phosphate metabolism
C52	Pc20g05830	gi|211587847	strong similarity to enoyl reductase of the lovastatin biosynthesis lovC - *Aspergillus terreus*	−4.0	3.0E-04	Reductase activity. Fatty acid biosynthesis
C53	Pc16g08460	gi|211585789	strong similarity to sorbitol dehydrogenase gutB - *Bacillus subtilis*	−3.3	4.6E-04	Carbohydrate Metabolism

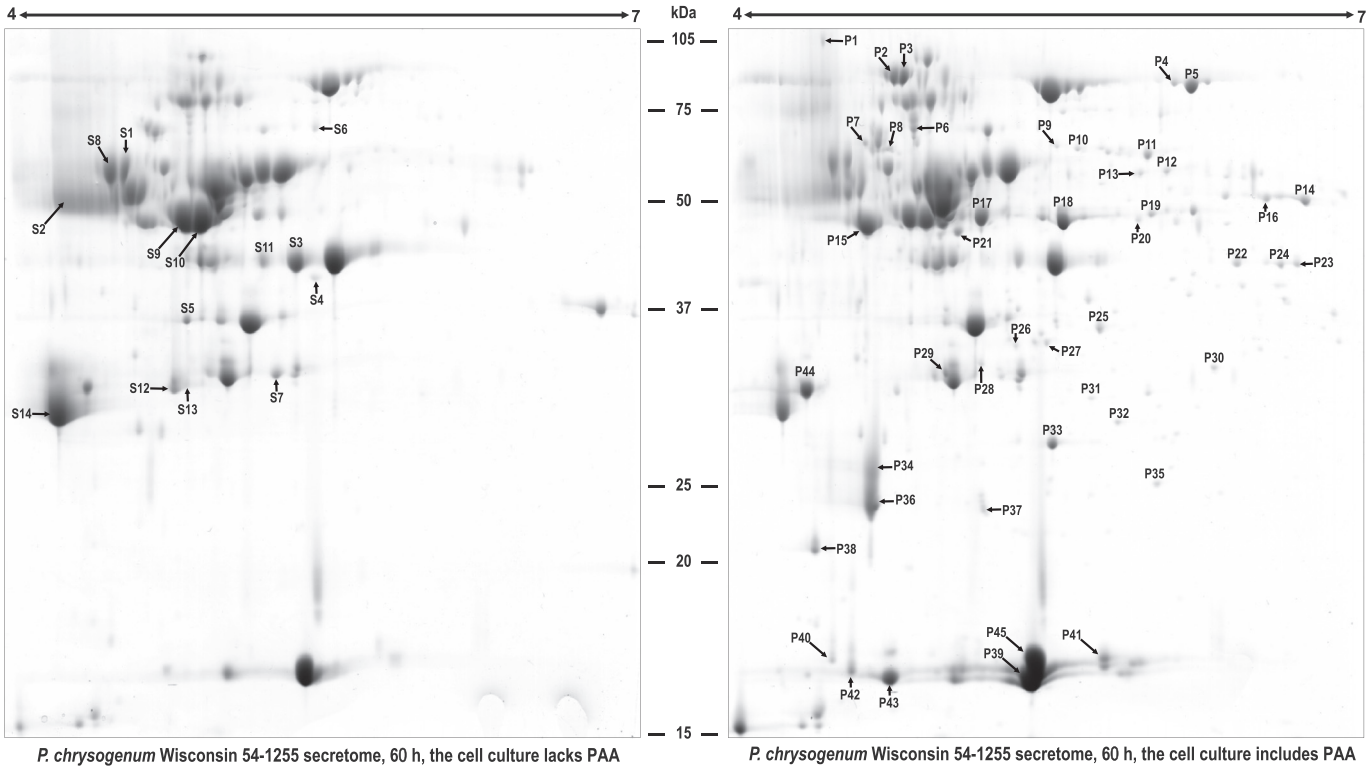

Fig. 7. Effect of phenylacetic acid (PAA) in the extracellular proteome of *P. rubens* (*P. chrysogenum* Wisconsin 54–1255). Extracellular proteins obtained from culture supernatants of *P. rubens* (*P. chrysogenum* Wisconsin 54–1255) grown for 60 h in DP medium with and without 1 g/L potassium phenylacetate, were separated by 2-DE using 18-cm wide-range IPG strips (pH 4–7 NL) and 12.5% SDS-PAGE gels, which were stained with CC following the "Blue Silver" staining method. Those spots overrepresented without PAA (underrepresented with PAA) are designated as "S", whereas the letter "P" was used to designate those spots overrepresented in the presence of PAA. The spots differentially represented in each condition are numbered and correspond to those proteins listed in Tables 3 ("P" spots) and 4 ("S" spots) and Supplementary Tables S3 ("P" spots) and S4 ("S" spots).

(Pc21g21370), which is directly involved in the last step of the penicillin biosynthetic pathway and catalyses the replacement of the IPN side chain by the aromatic aryl side chain provided by the activated form of phenylacetic acid (i.e. phenylacetyl CoA) [39]. Other important proteins are a hypothetical cystathionine beta synthase, which is involved in the biosynthesis of cystathionine, a precursor of the cysteine in the ACV tripeptide [40, 41], a probable ketol-acid reductoisomerase ilv-2 involved in step 2 of the subpathway that synthesizes L-valine (one of the three amino acid precursors of penicillin) from pyruvate, and a probable thioredoxin peroxidase (Pc22g04430), which together with thioredoxin and thioredoxin reductase, comprise the thioredoxin system involved in the reduction of bis-ACV (the oxidized disulfide form of ACV) and reincorporation of this molecule to the penicillin biosynthetic pathway [42]. S-adenosylmethionine synthase also resulted overrepresented after phenylacetate addition. This protein has been reported to coordinate fungal secondary metabolism and development [43] and its overexpression has been related to increased productivity of secondary metabolites in bacteria [44, 45].

When the extracellular protein fraction was analysed, we found some proteins lacking predicted signal sequences for secretion. This phenomenon has also been previously described in fungi [23, 46], pointing to these proteins as truly secreted multifunctional proteins with different activities according to their intracellular or extracellular location, a fact that has been confirmed in other organisms [47]. However, the extracellular presence of these proteins due to cell lysis events cannot be completely ruled out. One important mechanism involved in penicillin production and triggered by phenylacetic acid can be related to the induction and finding of the glutamate dehydrogenase (encoded by the *gdhA* gene) in the culture broths. Although this protein lacks classical or non-classical signal sequences for secretion, an extracellular form of glutamate dehydrogenase has been reported in other microorganisms, such as *Clostridium difficile*, where it confers resistance to hydrogen peroxide [48]. The protein encoded by the *gdhA* gene is NADPH-dependent and catalyses inside the cell the reductive amination of 2-oxoglutarate, thus giving rise to glutamate by means of a thermodynamically and energetically favored pathway for ammonium assimilation. Interestingly, the NADPH-dependent glutamate dehydrogenase has been reported to be involved in regulation of β-lactam production in industrial strains of *P. chrysogenum* [49] and therefore, its presence in the extracellular protein fraction in response to phenylacetic acid addition may represent important information for improved productivity.

5. Conclusions

These results provide important data about the fate of phenylacetic acid in *P. rubens*. In addition to being the side chain precursor of benzylpenicillin, this molecule also plays a positive role in penicillin production. This is achieved by means of the effect exerted on some proteins directly related to the biosynthesis of penicillin (IAT, thioredoxin peroxidase) and precursor amino acids (cystathionine beta synthase, ketol-acid reductoisomerase ilv-2), and other important proteins (NADPH-dependent glutamate dehydrogenase, S-adenosylmethionine synthase). This information contributes to the knowledge of the molecular mechanisms interconnected with phenylacetate utilization and penicillin biosynthesis in penicillin-producing strains of *P. rubens*.

Acknowledgments

This research was supported by Instituto de Competitividad Empresarial (ICE, formerly ADE) and Junta de Castilla y León. R. Domínguez-Santos was granted a fellowship from Junta de Castilla y

Table 3
Extracellular proteins overrepresented at 60 h in the presence of phenylacetic acid. Fold increase and p-value are indicated. Proteins that are only detected after the addition of phenylacetic acid are denoted as N/A.

Spot	ORF	Accession No	Similarity	Fold change	P-Value	Function	Signal peptide	Non-classically secreted protein
P1	Pc18g02900	gi|211586864	lysophospholipase phospholipase B plb1-Penicillium chrysogenum	N/A	N/A	Glycerophospholipid metabolism	YES	
P2	Pc22g06490	gi|211591694	strong similarity to alkaline phosphatase -Neurospora crassa	N/A	N/A	Dephosphorylation	YES	
P3	Pc22g06490	gi|211591694	strong similarity to alkaline phosphatase -Neurospora crassa	N/A	N/A	Dephosphorylation	YES	
P4	Pc22g02000	gi|211591261	strong similarity to mitochondrial aconitate hydratase Aco1 - Saccharomyces cerevisiae	N/A	N/A	Citric acid cycle	NO	NO
P5	Pc22g02000	gi|211591261	strong similarity to mitochondrial aconitate hydratase Aco1 - Saccharomyces cerevisiae	N/A	N/A	Citric acid cycle	NO	NO
P6	Pc22g09380	gi|211591967	strong similarity to glycosylphosphatidylinositol-anchored beta (1–3)glucanosyltransferase gel3 - Aspergillus fumigatus	3.7	1.0E-04	Cell wall morphogenesis	YES	
P7	Pc22g02800	gi|211591341	strong similarity to calcium-binding protein precursor cnx1p - Schizosaccharomyces pombe	N/A	N/A	Control of cellular functions	YES	
	Pc22g16510	gi|211592582	strong similarity to isoamyl alcohol oxidase mreA - Aspergillus oryzae	N/A	N/A	Formation of isovaleraldehyde	YES	
P8	Pc22g02800	gi|211591341	strong similarity to calcium-binding protein precursor cnx1p - Schizosaccharomyces pombe	N/A	N/A	Control of cellular functions	YES	
P9	Pc22g02000	gi|211591261	strong similarity to mitochondrial aconitate hydratase Aco1 - Saccharomyces cerevisiae	N/A	N/A	Citric acid cycle	NO	NO
P10	Pc22g22710	gi|211593182	strong similarity to dihydroxy-acid dehydratase Ilv3 - Saccharomyces cerevisiae	N/A	N/A	Biosynthesis of branched-chain amino acids	NO	YES
P11	Pc22g09390	gi|211591968	strong similarity to mannitol dehydrogenase mtlD - *Pseudomonas fluorescens*	N/A	N/A	Fructose and mannose metabolism	NO	NO
	Pc18g01390	gi|211586717	strong similarity to phosphoglucomutase pgmB - Aspergillus nidulans	N/A	N/A	Hexose metabolism	NO	YES
P12	Pc18g00980	gi|211586677	strong similarity to hypothetical trunk lateral cell specific gene HrTLC1 - Halocynthia roretzi	N/A	N/A	Redox metabolism	NO	YES
P13	Pc18g00980	gi|211586677	strong similarity to hypothetical trunk lateral cell specific gene HrTLC1 - Halocynthia roretzi	N/A	N/A	Redox metabolism	NO	YES
P14	Pc20g04720	gi|211587749	strong similarity to precursor of dihydrolipoamide dehydrogenase Lpd1 - Saccharomyces cerevisiae	N/A	N/A	E3 component of the pyruvate, α-ketoglutarate, and branched-chain amino acid-dehydrogenase complexes and the glycine cleavage system	NO	YES
P15	Pc18g01390	gi|211586717	strong similarity to phosphoglucomutase pgmB - Aspergillus nidulans	2.6	1.3E-06	Hexose metabolism	NO	YES
P16	Pc22g17560	gi|211592684	glutamate dehydrogenase gdhA-Penicillium chrysogenum	N/A	N/A	Ammonium utilization. Regulation of beta-lactam production	NO	NO
P17	Pc18g01390	gi|211586717	strong similarity to phosphoglucomutase pgmB - Aspergillus nidulans	3.4	1.8E-04	Hexose metabolism	NO	YES
P18	Pc14g01740	gi|211584789	enolase BAC82549-Penicillium chrysogenum	N/A	N/A	Glycolysis	NO	NO
P19	Pc20g03610	gi|211587647	strong similarity to precursor of mitochondrial isocitrate dehydrogenase icdA - Aspergillus niger	N/A	N/A	Citric acid cycle	NO	YES
P20	Pc16g05080	gi|211585478	strong similarity to adenosylhomocysteinase -Homo sapiens	N/A	N/A	Methylation cycle	NO	YES
P21	Pc12g14860	gi|211582909	extracellular acid phosphatase PhoA-Penicillium chrysogenum	16.1	3.5E-04	Dephosphorylation	YES	
P22	Pc12g04310	gi|211581920	strong similarity to acetate-inducible gene aciA - Aspergillus nidulans	N/A	N/A	Oxidation of formate. Formation of energy	NO	YES
P23	Pc12g04310	gi|211581920	strong similarity to acetate-inducible gene aciA - Aspergillus nidulans	N/A	N/A	Oxidation of formate. Formation of energy	NO	YES
P24	Pc16g02790	gi|211585272	strong similarity to aspartate transaminase like protein An08g01000 - Aspergillus niger	N/A	N/A	Amino acid metabolism	NO	YES
P25	Pc22g04850	gi|211591539	strong similarity to D-arabinose dehydrogenase Ara1 - Saccharomyces cerevisiae	N/A	N/A	Oxidoreductase activity	NO	NO
P26	Pc21g16950	gi|211590406	strong similarity to transaldolase Tal1 -Saccharomyces cerevisiae	N/A	N/A	Pentose phosphate pathway	NO	NO
P27	Pc21g16950	gi|211590406	strong similarity to transaldolase Tal1 -Saccharomyces cerevisiae	N/A	N/A	Pentose phosphate pathway	NO	NO
P28	Pc20g07230	gi|211587983	strong similarity to inorganic pyrophosphatase Ipp1 - Saccharomyces cerevisiae	N/A	N/A	General metabolism	NO	NO

(*continued on next page*)

Table 3 (*continued*)

Spot	ORF	Accession No	Similarity	Fold change	P-Value	Function	Signal peptide	Non-classically secreted protein
P29	Pc18g02740	gi|211586848	strong similarity to regucalcin also known as senescence marker protein-30 like protein An04g03420 -Aspergillus niger	N/A	N/A	Control of cellular functions	NO	NO
	Pc13g08730	gi|211583918	strong similarity to 1,3-beta-glucanosyltransferase bgt1 - Aspergillus fumigatus	N/A	N/A	Cell wall morphogenesis	YES	
P30	Pc12g05820	gi|211582045	strong similarity to esterase D ESD - Homo sapiens	N/A	N/A	General metabolism	NO	YES
P31	Pc13g04420	gi|211583497	orotidine 5-phosphate decarboxylase pyrG-Penicillium chrysogenum	N/A	N/A	Uridine biosynthesis	NO	YES
P32	Pc22g25470	gi|211593449	strong similarity to Sol1 - Saccharomyces cerevisiae	N/A	N/A	General metabolism	NO	YES
P33	Pc12g00830	gi|211581603	strong similarity to sorbitol utilization protein sou2 - Candida albicans	N/A	N/A	Carbohydrate Metabolism. (Related to short-chain alcohol dehydrogenases)	NO	NO
P34	Pc22g22290	gi|211593141	strong similarity to IgE-binding protein -Aspergillus fumigatus	N/A	N/A	Unknown	YES	
P35	Pc12g00830	gi|211581603	strong similarity to sorbitol utilization protein sou2 - Candida albicans	N/A	N/A	Carbohydrate Metabolism. (Related to short-chain alcohol dehydrogenases)	NO	NO
P36	Pc12g13600	gi|211582786	strong similarity to hypothetical necrosis and ethylene inducing protein BH0395 - Bacillus halodurans	N/A	N/A	Produces Immune responses and cell death in plants	YES	
	Pc22g22290	gi|211593141	strong similarity to IgE-binding protein -Aspergillus fumigatus	N/A	N/A	Unknown	YES	
P37	Pc20g04810	gi|211587757	strong similarity to estrogen receptor-binding cyclophilin cypD - Bos primigenius taurus	N/A	N/A	Control of cellular functions	NO	NO
P38	Pc21g14220	gi|211590148	strong similarity to hypothetical protein contig1495_2.tfa_630cg - Aspergillus fumigatus	N/A	N/A	Unknown	YES	
P39	Pc21g12590	gi|211589997	similarity to 6-hydroxy-D-nicotine oxidase 6-HDNO - Arthrobacter oxidans	N/A	N/A	Oxidoreductase activity	YES	
	Pc21g02110	gi|211588987	strong similarity to hypothetical protein mg01387.1 - Magnaporthe grisea	N/A	N/A	Unknown	YES	
P40	Pc12g10010	gi|211582445	strong similarity to protein copper regulated - Aspergillus nidulans	N/A	N/A	Unknown	YES	
P41	Pc22g09680	gi|211591995	similarity to hypothetical protein PA4204 - Pseudomonas aeruginosa	9.9	6.3E-05	Unknown	YES	
P42		gi|144,952,798	16 kDa allergen [Penicillium chrysogenum]	N/A	N/A	Unknown	YES	
P43	Pc14g01740	gi|211584789	enolase BAC82549-Penicillium chrysogenum	11.5	4.3E-06	Glycolysis	NO	NO
P44	Pc22g05880	gi|211591637	strong similarity to hypothetical protein 1117_scaffold_1.tfa_300cg - Fusarium graminearum	2.3	2.8E-04	Unknown	YES	
P45	Pc22g00190	gi|211591082	strong similarity to hypothetical cell wall protein binB - Aspergillus nidulans	N/A	N/A	Unknown	YES	

Table 4
Extracellular proteins underrepresented at 60 h in the presence of phenylacetic acid. Fold decrease and p-value are indicated. Proteins that are not detected after the addition of phenylacetic acid are denoted as N/A.

Spot	ORF	Accession No	Similarity	Fold change	P-Value	Function	Signal peptide	Non-classically secreted protein
S1	Pc22g17870	gi|211592713	strong similarity to hypothetical ECM33 homolog SPCC1223.12c - Schizosaccharomyces pombe	−2.9	5.4E-06	Unknown	YES	
S2	Pc21g23210	gi|211590999	strong similarity to cell wall protein Crh1 -Saccharomyces cerevisiae	−4.6	7.1E-04	Cell wall morphogenesis	YES	
S3	Pc22g20290	gi|211592946	strong similarity to polygalacturonase pgaI -Aspergillus niger	−6.3	4.2E-05	Plant cell wall degradation	YES	
S4	Pc22g13130	gi|211592257	strong similarity to mitochondrial aspartate aminotransferase mAspAT - Mus musculus	−3.6	4.0E-05	Amino acid metabolism	NO	YES
S5	Pc22g24890	gi|211593394	strong similarity to pectate lyase plyA -Aspergillus niger	−5.0	4.7E-05	Plant cell wall degradation	YES	
	Pc12g07820	gi|211582235	similarity to chitosanase csnA - Aspergillus oryzae	−5.0	4.7E-05	Cell wall morphogenesis	YES	
	Pc20g07020	gi|211587962	endo-1,4-beta-xylanase A precursor XylP-Penicillium chrysogenum	−5.0	4.7E-05	Plant cell wall degradation	YES	
S6	Pc12g13400	gi|211582767	strong similarity to cephalosporin esterase -*Rhodosporidium toruloides*	−5.2	1.4E-03	Esterase activity	YES	
S7	Pc12g01330	gi|211581651	strong similarity to hypothetical protein contig31_part_ii.tfa_1360wg - Aspergillus fumigatus	−8.0	1.3E-04	Unknown	YES	
S8	Pc22g17870	gi|211592713	strong similarity to hypothetical ECM33 homolog SPCC1223.12c - Schizosaccharomyces pombe	−2.0	6.5E-05	Unknown	YES	
S9	Pc22g22810	gi|211593192	strong similarity to sulphydryl oxidase Sox from patent EP565172-A1 - Aspergillus niger	−2.0	6.3E-04	Oxidation of sulfhydryl compounds	YES	
S10	Pc22g22810	gi|211593192	strong similarity to sulphydryl oxidase Sox from patent EP565172-A1 - Aspergillus niger	−2.2	4.9E-03	Oxidation of sulfhydryl compounds	YES	
S11	Pc22g20290	gi|211592946	strong similarity to polygalacturonase pgaI -Aspergillus niger	N/A	N/A	Plant cell wall degradation	YES	
S12	Pc20g07030	gi|211587963	strong similarity to 1,4-beta-Δ-arabinoxylan arabinofuranohydrolase axhA - Aspergillus niger	−6.9	1.6E-03	Plant cell wall degradation	YES	
S13	Pc20g07030	gi|211587963	strong similarity to 1,4-beta-Δ-arabinoxylan arabinofuranohydrolase axhA - Aspergillus niger	N/A	N/A	Plant cell wall degradation	YES	
S14	Pc06g00430	gi|211581271	strong similarity to ribonuclease T2 precursor rntB - Aspergillus oryzae	−2.7	9.2E-03	Ribonuclease activity	YES	

León (ORDEN EDU/1204/2010) co-financed by the Fondo Social Europeo. M.F. Vasco-Cárdenas was granted a MAEC-AECID (II.E) fellowship from Ministry of Foreign Affairs through the Spanish Agency for International Cooperation (AECID). Authors wish to thank B. Martín, J. Merino, C. Sánchez and C. Rodríguez for their excellent technical assistance.

Appendix A. Supplementary data

Supplementary data to this article can be found online at https://doi.org/10.1016/j.jprot.2018.08.006.

References

[1] G. Hersbach, C. Van der Beek, P. Van Dijck, The penicillins: properties, biosynthesis, and fermentation, in: E. Vandamme (Ed.), Biotechnol. Ind. Antibiot. Drugs Pharm. Sci, Vol. 22 Marcel Dekker, New York, 1984, pp. 45–140.
[2] J. Houbraken, J.C. Frisvad, R.A. Samson', Fleming's penicillin producing strain is not *Penicillium chrysogenum* but *P. rubens*, IMA Fungus 2 (2011) 87–95, https://doi.org/10.5598/imafungus.2011.02.01.12.
[3] J. Martín, P. Liras, Insights into the structure and molecular mechanisms of β-lactam synthesizing enzymes in fungi, in: G. Brahmachati, A. Demain, J. Adrio (Eds.), Biotechnology of Microbial Enzymes, Elsevier, NewYork, 2016, pp. 215–241.
[4] J.F. Martín, R.V. Ullán, C. García-Estrada, Regulation and compartmentalization of β-lactam biosynthesis, Microb. Biotechnol. 3 (2010) 285–299, https://doi.org/10.1111/j.1751-7915.2009.00123.x.
[5] C. García-Estrada, J.-F. Martín, Penicillins, in: J.F. Martin, C. García-Estrada, S. Zeilinger (Eds.), Biosynthesis and Molelcular Genetics of Fungal Secondary Metabolism, vol I, Springer US, New York, 2014, pp. 17–42.
[6] M. Lamas-Maceiras, I. Vaca, E. Rodríguez, J. Casqueiro, J.F. Martín, Amplification and disruption of the phenylacetyl-CoA ligase gene of Penicillium chrysogenum encoding an aryl-capping enzyme that supplies phenylacetic acid to the isopenicillin N-acyltransferase, Biochem. J. 395 (2006) 147–155, https://doi.org/10.1042/BJ20051599.
[7] F.-Q. Wang, J. Liu, M. Dai, Z.-H. Ren, C.-Y. Su, J.-G. He, Molecular cloning and functional identification of a novel phenylacetyl-CoA ligase gene from Penicillium chrysogenum, Biochem. Biophys. Res. Commun. 360 (2007) 453–458, https://doi.org/10.1016/j.bbrc.2007.06.074.
[8] M.J. Koetsier, A.K. Gombert, S. Fekken, R.A.L. Bovenberg, M.A. van den Berg, J.A.K.W. Kiel, P.A. Jekel, D.B. Janssen, J.T. Pronk, I.J. van der Klei, J.-M. Daran, The Penicillium chrysogenum aclA gene encodes a broad-substrate-specificity acyl-coenzyme A ligase involved in activation of adipic acid, a side-chain precursor for cephem antibiotics, Fungal Genet. Biol. 47 (2010) 33–42, https://doi.org/10.1016/j.fgb.2009.10.003.
[9] Z.-L. Yu, J. Liu, F.-Q. Wang, M. Dai, B.-H. Zhao, J.-G. He, H. Zhang, Cloning and characterization of a novel CoA-ligase gene from Penicillium chrysogenum, Folia Microbiol. Praha 56 (2011) 246–252, https://doi.org/10.1007/s12223-011-0044-y.
[10] F. Fierro, J.L. Barredo, B. Díez, S. Gutierrez, F.J. Fernández, J.F. Martín, The penicillin gene cluster is amplified in tandem repeats linked by conserved hexanucleotide sequences, Proc. Natl. Acad. Sci. U. S. A. 92 (1995) 6200–6204 http://www.ncbi.nlm.nih.gov/pubmed/7597101 , Accessed date: 12 May 2018.
[11] W.H. Müller, T.P. van der Krift, A.J. Krouwer, H.A. Wösten, L.H. van der Voort, E.B. Smaal, A.J. Verkleij, Localization of the pathway of the penicillin biosynthesis in Penicillium chrysogenum, EMBO J. 10 (1991) 489–495 http://www.ncbi.nlm.nih.gov/pubmed/1899377 , Accessed date: 12 May 2018.
[12] M.A. van den Berg, R. Albang, K. Albermann, J.H. Badger, J.-M. Daran, A.J.M. Driessen, C. Garcia-Estrada, N.D. Fedorova, D.M. Harris, W.H.M. Heijne, V. Joardar, J.A.K.W. Kiel, A. Kovalchuk, J.F. Martín, W.C. Nierman, J.G. Nijland, J.T. Pronk, J.A. Roubos, I.J. van der Klei, N.N.M.E. van Peij, M. Veenhuis, H. von Döhren, C. Wagner, J. Wortman, R.A.L. Bovenberg, Genome sequencing and analysis of the filamentous fungus Penicillium chrysogenum, Nat. Biotechnol. 26 (2008) 1161–1168, https://doi.org/10.1038/nbt.1498.
[13] M.-S. Jami, C. Barreiro, C. García-Estrada, J.-F. Martín, Proteome analysis of the penicillin producer Penicillium chrysogenum: characterization of protein changes during the industrial strain improvement, Mol. Cell. Proteomics 9 (2010) 1182–1198, https://doi.org/10.1074/mcp.M900327-MCP200.
[14] M. Rodríguez-Sáiz, J.L. Barredo, M.A. Moreno, J.M. Fernández-Cañón, M.A. Peñalva, B. Díez, Reduced function of a phenylacetate-oxidizing cytochrome p450 caused strong genetic improvement in early phylogeny of penicillin-producing strains, J. Bacteriol. 183 (2001) 5465–5471, https://doi.org/10.1128/JB.183.19.5465-5471.2001.
[15] M. Rodríguez-Sáiz, B. Díez, J.L. Barredo, Why did the Fleming strain fail in penicillin industry? Fungal Genet. Biol. 42 (2005) 464–470, https://doi.org/10.1016/j.fgb.2005.01.014.
[16] J.M. Fernández-Cañón, M.A. Peñalva, Molecular characterization of a gene encoding a homogentisate dioxygenase from aspergillus nidulans and identification of its human and plant homologues, J. Biol. Chem. 270 (1995) 21199–21205 http://www.ncbi.nlm.nih.gov/pubmed/7673153 , Accessed date: 12 May 2018.
[17] J.M. Fernández-Cañón, M.A. Peñalva, Fungal metabolic model for human type I hereditary tyrosinaemia, Proc. Natl. Acad. Sci. U. S. A. 92 (1995) 9132–9136 http://www.ncbi.nlm.nih.gov/pubmed/7568087 , Accessed date: 12 May 2018.

[18] J.M. Mingot, M.A. Peñalva, J.M. Fernández-Cañón, Disruption of phacA, an aspergillus nidulans gene encoding a novel cytochrome P450 monooxygenase catalyzing phenylacetate 2-hydroxylation, results in penicillin overproduction, J. Biol. Chem. 274 (1999) 14545–14550 http://www.ncbi.nlm.nih.gov/pubmed/10329644 , Accessed date: 12 May 2018.
[19] E. Arias-Barrau, E.R. Olivera, J.M. Luengo, C. Fernández, B. Galán, J.L. García, E. Díaz, B. Miñambres, The homogentisate pathway: a central catabolic pathway involved in the degradation of L-phenylalanine, L-tyrosine, and 3-hydroxyphenylacetate in Pseudomonas putida, J. Bacteriol. 186 (2004) 5062–5077, https://doi.org/10.1128/JB.186.15.5062-5077.2004.
[20] F. Ferrer-Sevillano, J.M. Fernández-Cañón, Novel phacB-encoded cytochrome P450 monooxygenase from aspergillus nidulans with 3-hydroxyphenylacetate 6-hydroxylase and 3,4-dihydroxyphenylacetate 6-hydroxylase activities, Eukaryot. Cell 6 (2007) 514–520, https://doi.org/10.1128/EC.00226-06.
[21] T. Veiga, D. Solis-Escalante, G. Romagnoli, A. ten Pierick, M. Hanemaaijer, A.T. Deshmukh, A. Deshmuhk, A. Wahl, J.T. Pronk, J.-M. Daran, Resolving phenylalanine metabolism sheds light on natural synthesis of penicillin G in Penicillium chrysogenum, Eukaryot. Cell 11 (2012) 238–249, https://doi.org/10.1128/EC.05285-11.
[22] D.M. Harris, Z.A. van der Krogt, P. Klaassen, L.M. Raamsdonk, S. Hage, M.A. van den Berg, R.A.L. Bovenberg, J.T. Pronk, J.-M. Daran, Exploring and dissecting genome-wide gene expression responses of Penicillium chrysogenum to phenylacetic acid consumption and penicillinG production, BMC Genomics 10 (2009) 75, https://doi.org/10.1186/1471-2164-10-75.
[23] M.-S. Jami, C. García-Estrada, C. Barreiro, A.-A. Cuadrado, Z. Salehi-Najafabadi, J.-F. Martín, The Penicillium chrysogenum extracellular proteome. Conversion from a food-rotting strain to a versatile cell factory for white biotechnology, Mol. Cell. Proteomics 9 (2010) 2729–2744, https://doi.org/10.1074/mcp.M110.001412.
[24] J. Casqueiro, O. Bañuelos, S. Gutiérrez, M.J. Hijarrubia, J.F. Martín, Intrachromosomal recombination between direct repeats in Penicillium chrysogenum: gene conversion and deletion events, Mol Gen Genet 261 (1999) 994–1000 http://www.ncbi.nlm.nih.gov/pubmed/10485291 , Accessed date: 12 May 2018.
[25] C. García-Estrada, R.V. Ullán, T. Velasco-Conde, R.P. Godio, F. Teijeira, I. Vaca, R. Feltrer, K. Kosalková, E. Mauriz, J.F. Martín, Post-translational enzyme modification by the phosphopantetheinyl transferase is required for lysine and penicillin biosynthesis but not for roquefortine or fatty acid formation in Penicillium chrysogenum, Biochem. J. 415 (2008) 317–324, https://doi.org/10.1042/BJ20080369.
[26] R.V. Ullán, R.P. Godio, F. Teijeira, I. Vaca, C. García-Estrada, R. Feltrer, K. Kosalkova, J.F. Martín, RNA-silencing in Penicillium chrysogenum and Acremonium chrysogenum: validation studies using beta-lactam genes expression, J. Microbiol. Methods 75 (2008) 209–218, https://doi.org/10.1016/j.mimet.2008.06.001.
[27] J.M. Cantoral, B. Díez, J.L. Barredo, E. Alvarez, J.F. Martín, High–frequency transformation of Penicillium chrysogenum, Nat. Biotechnol. 5 (1987) 494–497, https://doi.org/10.1038/nbt0587-494.
[28] F. Fierro, C. García-Estrada, N.I. Castillo, R. Rodríguez, T. Velasco-Conde, J.-F. Martín, Transcriptional and bioinformatic analysis of the 56.8 kb DNA region amplified in tandem repeats containing the penicillin gene cluster in Penicillium chrysogenum, Fungal Genet. Biol. 43 (2006) 618–629, https://doi.org/10.1016/j.fgb.2006.03.001.
[29] C. García-Estrada, I. Vaca, M. Lamas-Maceiras, J.F. Martín, In vivo transport of the intermediates of the penicillin biosynthetic pathway in tailored strains of Penicillium chrysogenum, Appl. Microbiol. Biotechnol. 76 (2007) 169–182, https://doi.org/10.1007/s00253-007-0999-4.
[30] G. Candiano, M. Bruschi, L. Musante, L. Santucci, G.M. Ghiggeri, B. Carnemolla, P. Orecchia, L. Zardi, P.G. Righetti, Blue silver: a very sensitive colloidal Coomassie G-250 staining for proteome analysis, Electrophoresis 25 (2004) 1327–1333, https://doi.org/10.1002/elps.200305844.
[31] J. Havlis, H. Thomas, M. Sebela, A. Shevchenko, Fast-response proteomics by accelerated in-gel digestion of proteins, Anal. Chem. 75 (2003) 1300–1306 http://www.ncbi.nlm.nih.gov/pubmed/12659189 , Accessed date: 12 May 2018.
[32] A.J. Moyer, R.D. Coghill, Penicillin: X. The effect of phenylacetic acid on Penicillin production, J. Bacteriol. 53 (1947) 329–341 http://www.ncbi.nlm.nih.gov/pubmed/16561276 , Accessed date: 12 May 2018.
[33] S. Subramani, Protein import into peroxisomes and biogenesis of the organelle, Annu. Rev. Cell Biol. 9 (1993) 445–478, https://doi.org/10.1146/annurev.cb.09.110193.002305.
[34] J.-F. Martín, C. García-Estrada, R.V. Ullán, Transport of substrates into peroxisomes: the paradigm of β-lactam biosynthetic intermediates, Biomol. Concepts 4 (2013) 197–211, https://doi.org/10.1515/bmc-2012-0048.
[35] J.M. Fernández-Cañón, A. Reglero, H. Martínez-Blanco, M.A. Ferrero, J.M. Luengo, Phenylacetic acid transport system in Penicillium chrysogenum Wis 54–1255: molecular specificity of its induction, J. Antibiot. Tokyo 42 (1989) 1410–1415 http://www.ncbi.nlm.nih.gov/pubmed/2507494 , Accessed date: 12 May 2018.
[36] J.M. Fernández-Cañón, A. Reglero, H. Martínez-Blanco, J.M. Luengo, Uptake of phenylacetic acid by Penicillium chrysogenum Wis 54–1255: a critical regulatory point in benzylpenicillin biosynthesis, J. Antibiot. Tokyo 42 (1989) 1398–1409 http://www.ncbi.nlm.nih.gov/pubmed/2507493 , Accessed date: 12 May 2018.
[37] D.J. Hillenga, H. Versantvoort, S. van der Molen, A. Driessen, W.N. Konings, Penicillium chrysogenum takes up the penicillin G precursor Phenylacetic acid by passive diffusion, Appl. Environ. Microbiol. 61 (1995) 2589–2595 http://www.ncbi.nlm.nih.gov/pubmed/16535072 , Accessed date: 12 May 2018.
[38] M. Fernández-Aguado, R.V. Ullán, F. Teijeira, R. Rodríguez-Castro, J.F. Martín, The transport of phenylacetic acid across the peroxisomal membrane is mediated by the PaaT protein in Penicillium chrysogenum, Appl. Microbiol. Biotechnol. 97 (2013) 3073–3084, https://doi.org/10.1007/s00253-012-4425-1.
[39] E. Alvarez, B. Meesschaert, E. Montenegro, S. Gutiérrez, B. Díez, J.L. Barredo, J.F. Martín, The isopenicillin-N acyltransferase of Penicillium chrysogenum has isopenicillin-N amidohydrolase, 6-aminopenicillanic acid acyltransferase and penicillin amidase activities, all of which are encoded by the single penDE gene, Eur. J. Biochem. 215 (1993) 323–332 http://www.ncbi.nlm.nih.gov/pubmed/8344300 , Accessed date: 12 May 2018.
[40] K. Kosalková, A.T. Marcos, J.F. Martín, A moderate amplification of the mecB gene encoding cystathionine-gamma-lyase stimulates cephalosporin biosynthesis in Acremonium chrysogenum, J. Ind. Microbiol. Biotechnol. 27 (2001) 252–258, https://doi.org/10.1038/sj/jim/7000192.
[41] J.F. Martín, A.L. Demain, Unraveling the methionine-cephalosporin puzzle in Acremonium chrysogenum, Trends Biotechnol. 20 (2002) 502–507 http://www.ncbi.nlm.nih.gov/pubmed/12443871 , Accessed date: 12 May 2018.
[42] G. Cohen, A. Argaman, R. Schreiber, M. Mislovati, Y. Aharonowitz, The thioredoxin system of Penicillium chrysogenum and its possible role in penicillin biosynthesis, J. Bacteriol. 176 (1994) 973–984 http://www.ncbi.nlm.nih.gov/pubmed/8106340 , Accessed date: 12 May 2018.
[43] J. Gerke, O. Bayram, G.H. Braus, Fungal S-adenosylmethionine synthetase and the control of development and secondary metabolism in Aspergillus nidulans, Fungal Genet. Biol. 49 (2012) 443–454, https://doi.org/10.1016/j.fgb.2012.04.003.
[44] S. Okamoto, A. Lezhava, T. Hosaka, Y. Okamoto-Hosoya, K. Ochi, Enhanced expression of S-adenosylmethionine synthetase causes overproduction of actinorhodin in Streptomyces coelicolor A3(2), J. Bacteriol. 185 (2003) 601–609 http://www.ncbi.nlm.nih.gov/pubmed/12511507 , Accessed date: 12 May 2018.
[45] X.Q. Zhao, B. Gust, L. Heide, S-Adenosylmethionine (SAM) and antibiotic biosynthesis: effect of external addition of SAM and of overexpression of SAM biosynthesis genes on novobiocin production in Streptomyces, Arch. Microbiol. 192 (2010) 289–297, https://doi.org/10.1007/s00203-010-0548-x.
[46] P. Shah, J.A. Atwood, R. Orlando, H. El Mubarek, G.K. Podila, M.R. Davis, Comparative proteomic analysis of *Botrytis cinerea* Secretome, J. Proteome Res. 8 (2009) 1123–1130, https://doi.org/10.1021/pr8003002.
[47] S. McGoldrick, S.M. O'Sullivan, D. Sheehan, Glutathione transferase-like proteins encoded in genomes of yeasts and fungi: insights into evolution of a multifunctional protein superfamily, FEMS Microbiol. Lett. 242 (2005) 1–12, https://doi.org/10.1016/j.femsle.2004.10.033.
[48] B.P. Girinathan, S.E. Braun, R. Govind, Clostridium difficile glutamate dehydrogenase is a secreted enzyme that confers resistance to H2O2, Microbiology 160 (2014) 47–55, https://doi.org/10.1099/mic.0.071365-0.
[49] J. Thykaer, K. Rueksomtawin, H. Noorman, J. Nielsen, NADPH-dependent glutamate dehydrogenase in Penicillium chrysogenum is involved in regulation of beta-lactam production, Microbiology 154 (2008) 1242–1250, https://doi.org/10.1099/mic.0.2007/010017-0.